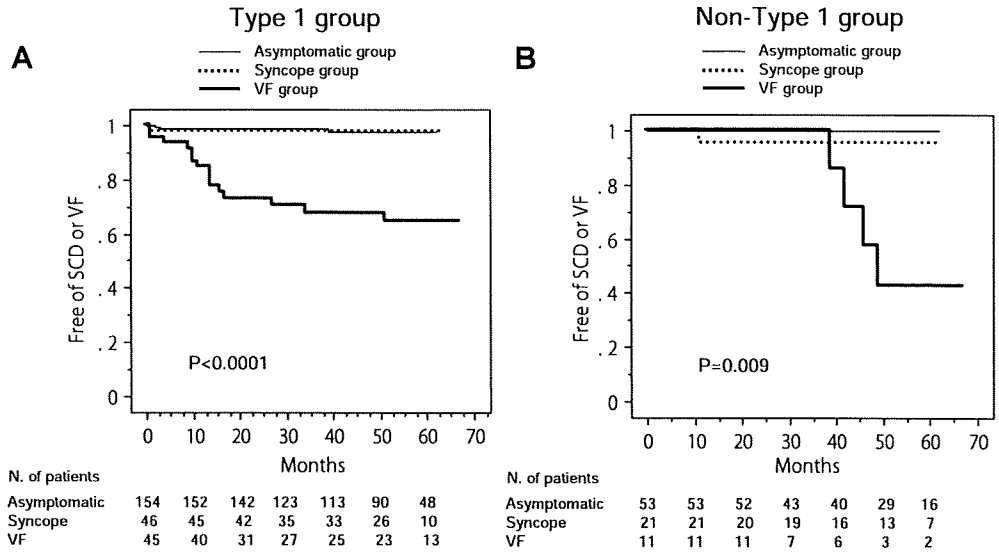

Figure 4. Kaplan–Meier analysis of arrhythmic events (SCD or documented VF) during follow-up depending on the clinical presentation (VF/aborted sudden death, syncope, or asymptomatic) in probands with type 1 ECG (A) and those with non–type 1 ECG (B). $P<0.0001$ represents overall comparison, and $P=0.009$ is for comparison between the VF group and the syncope group. There was no statistically significant difference ($P=0.95$) in the events-free survival of VF probands comparing type 1 and non–type 1 groups.

annual rate of arrhythmic events in probands with type 1 ECG was 10.2% in the VF group, 0.6% in the syncope group, and 0.5% in the asymptomatic group (Figure 4A). The cumulative rate of arrhythmic events in probands with non–type 1 ECG was similar to those with type 1 ECG. The annual arrhythmic event rate was 10.6%, 1.2%, and 0%, respectively (Figure 4B).

By univariate analysis, a family history of SCD was a predictor for arrhythmic events in the type 1 group (hazard ratio [HR], 5.1; 95% CI, 2.0 to 12.8; $P=0.0004$) and the non–type 1 group (HR, 12.3; 95% CI, 2.0 to 74.8; $P=0.006$). Coexistence of posterolateral early repolarization with precordial Brugada-pattern ECG was another predictor in the type 1 group (HR, 4.2; 95% CI, 1.6 to 11.2; $P=0.003$); however, other parameters were not reliable. Figure 5 shows the Kaplan–Meier curves of arrhythmic events in the type 1 group during follow-up, depending on the presence of a family history of SCD (Figure 5A), inferolateral early repolarization (Figure 5B), a spontaneous type 1 ST-elevation (Figure 5C), and inducibility of ventricular arrhythmias by EPS (Figure 5D). Multivariate analysis in all probands identified that the former 2 parameters were independent risk factors for arrhythmic events (a family history of SCD: HR, 3.28; 95% CI, 1.42 to 7.60; $P=0.005$; early repolarization: HR, 2.66; 95% CI, 1.06 to 6.71; $P=0.03$, Table 3) as well as a family history of SCD in analysis of probands without VF (syncope and asymptomatic groups) (HR, 12.5; 95% CI, 2.0 to 75.0; $P=0.005$).

Discussion

Main Findings

We present one of the largest series of consecutive patients with Brugada-pattern ECG. Importantly, in the present study only probands were included. Also, this study has the longest follow-up ever reported. The main finding is that probands who have a non–type 1 ECG, even after challenged with a sodium channel blocker, do not necessarily have a better prognosis than patients with spontaneous or drug-induced type 1 ECG. Patients presenting with aborted cardiac arrest had a grim prognosis and those presenting with syncope or no symptoms had an excellent prognosis irrespective of their ECG pattern (that is, type 1 versus non–type 1). Also, a family history of sudden death at age <45 years and coexistence of early repolarization in the inferolateral leads were predictors of poor outcome. In contrast, VF/VT inducibility during EPS was not a predictor of outcome.

Comparison With Previous Studies

In this study, the follow-up time was uniform among the 3 groups. The mean follow-up time for the asymptomatic individuals was the longest (47.7±15.0 months) compared with the studies by Brugada et al[2] (27±29 months), Priori et al[3] (34±44 months), and Eckardt et al[5] (33.7±52.2 months). The percentage of female patients (5%) and patients with a family history of SCD (14%) was significantly smaller than 2 of these previous reports (5% versus 24% to 28%[2,3,5]; $P<0.001$, and 14% versus 28% to 54%[2,3,5]; $P<0.001$), although the percentage (14%) of a family history of SCD was similar to that of probands (20%) that Priori et al[3] had reported. The values observed in the present study may reflect the true profile of the probands of Brugada syndrome in contrast to previous studies in which a significant number of family members were also enrolled.

Prognosis of Probands Presenting With Syncope and Without Symptoms

The prognosis of probands in the syncope and asymptomatic groups was very good, and the annual rate of arrhythmic events was ≤1.2%. In the syncope group, this rate is far less than reported in previous studies,[2–5] although the

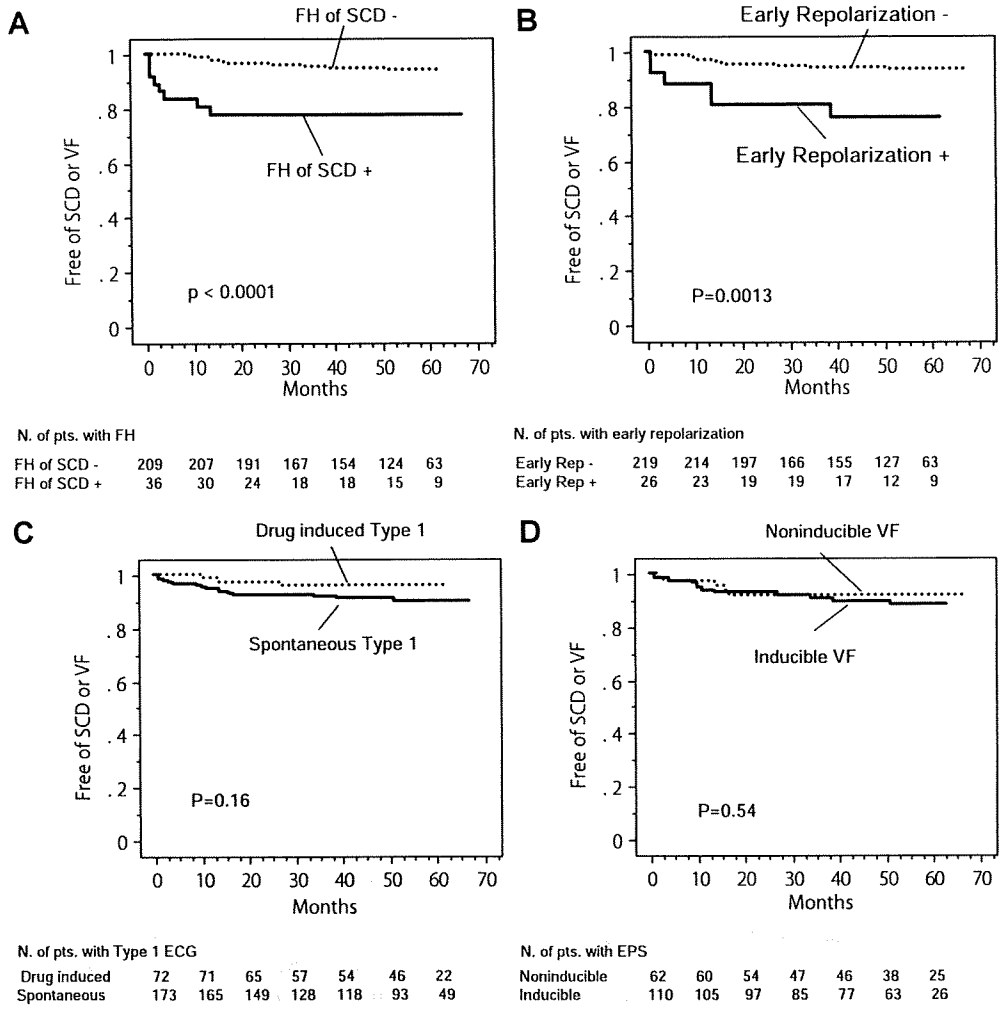

Figure 5. Kaplan–Meier analysis of fatal arrhythmic events during follow-up depending on a family history (FH) of SCD (FH of SCD− versus FH of SCD +) (A), inferolateral early repolarization (early repolarization− versus early repolarization+) (B), a spontaneous type 1 ST-elevation (drug-induced type 1 versus spontaneous type 1) (C), and inducibility of ventricular arrhythmias by EPS (noninducible VF versus inducible VF) (D).

rate in the asymptomatic group is similar to that in the Eckardt registry[5] and the rate of around 10% for the VF group is comparable to the rate reported in the Brugada registries.[2,8] The reason that the patients in the syncope group showed excellent prognosis is not entirely clear but may be related to the method of registry. Poor prognosis in prior studies is possibly related to the retrospective design of the studies consisting of probands and family members,[2,3,5] in which only severe syncope directly linked to VF tends to be categorized later as a syncope, despite difficulty to determine the cause of syncope at the onset. Even so, we cannot exclude the possibility that some patients with vasovagal syncope were inevitably included in the syncope group because not a few patients have undefined syncope and >30% of Brugada patients are reported to have both vasovagal syncope and the syncope due to ventricular arrhythmia.[12] Another reason for the good prognosis is the difference of genetic background. Brugada syndrome is known to be common in Asian people, which possibly relates to the higher prevalence of polymorphism of haplotype B, associated with the cardiac sodium channel.[13,14] The average prognosis of Asian patients with Brugada syndrome may be better than that of the white population, because individuals without a critical genetic defect are easily detected as a Brugada patient in a routine medical checkup. Further genetic studies are required to clarify the racial difference of outcome. Nevertheless, the patients in this study with an aborted sudden death showed worse prognosis than European people in the study by Eckardt et al[5] and had a similar outcome to those who underwent ICD implantation.[15]

Prognosis of Probands With Non–Type 1 ECG

The outcome of probands with non–type 1 ECG was similar to those with type 1 ECG and the rate of arrhythmic events in the VF group was considerably higher. Some of these patients had shown a coved (type 1) ST-elevation only in the higher (second or third) intercostal spaces during the drug provocation test or follow-up. Miyamoto et al[16] reported that men with a spontaneous type 1 ECG

Table 3. Probability of Sudden Death or VF During Follow-Up Depending on Clinical and Electrophysiological Variables in All Probands (Type 1 and Non–Type 1 Groups)

	Univariate Analysis			Multivariate Analysis		
	HR	95% CI	*P* Value	HR	95% CI	*P* Value
Prior VF	21.46	8.00–57.53	<0.0001	17.48	6.22–49.11	<0.0001
FH of SCD	6.35	2.84–14.19	<0.0001	3.28	1.42–7.60	0.005
Inferolateral ER	4.14	1.71–10.00	0.001	2.66	1.06–6.71	0.03
AF	2.15	0.92–5.03	0.07	0.87	0.36–2.09	0.75
Syncope	0.35	0.08–1.09	0.15			
Sp. type1	2.31	0.67–7.94	0.18			
VF induc. (apex/OT)	1.81	0.72–4.70	0.20			
VF induc. (apex)	1.58	0.60–4.11	0.34			
Male		NA				

FH indicates family history; inferolateral ER, inferolateral early repolarization; AF, atrial fibrillation; Sp. type 1, spontaneous type 1 ST-elevation on 12-lead ECG at baseline; VF induc. (apex/OT), VF induction by programmed pacing at the RV apex or RV outflow tract; and VF induc. (apex), VF induction by programmed pacing at the RV apex.

recorded only at the higher leads V_1 and V_2 showed a prognosis similar to that of men with a type 1 ECG when using standard leads. In the past, patients with non–type 1 ST-elevation in standard ECG had been excluded from studies as a benign entity of Brugada syndrome. However, if patients had a history of aborted sudden death or agonizing nocturnal dyspnea, non–type 1 Brugada-pattern ECG should not be disregarded. Careful follow-up including ECG recording at the higher intercostals spaces and the implantation of ICD is probably required in such a patient to prevent SCD.

Clinical Features of Probands With Non–Type 1 ECG

The clinical profiles of probands were very similar between the non–type 1 group and the type 1 group (Table 2). Inferolateral early repolarization occurred equally in small percentage of patients in both groups (8% and 11%, respectively), which is comparable to the prevalence (12%) of early repolarization that Letsas et al[17] reported in patients with Brugada syndrome. This means that the patient characteristics of the non–type 1 group are much closer to Brugada syndrome than early repolarization syndrome reported by Haïssaguerre et al,[9] in which the VF occurrence rate during sleeping was low (19%) and VF inducibility by EPS was only 34%. Moreover, they reported that several aspects including the relapsing VF and the efficacy of isoproterenol and quinidine,[9,18] which were observed in some patients with early repolarization, were exactly like those of typical Brugada syndrome. Haïssaguerre et al[9] excluded patients with Brugada syndrome, defined as right bundle-branch block and ST-segment elevation >0.2mV in leads V_1–V_3, at the enrollment. However, considering that they possibly included patients with non–type 1 ECG as non-Brugada pattern in their study, some patients with prior VF and early repolarization might have represented non–type 1 Brugada patients of high risk.

Predictors of Outcome

It was reported that male sex, a previous episode of syncope, a spontaneous type 1 ECG, and inducibility of ventricular arrhythmias by EPS are predictors for poor outcome.[2–4] Brugada et al demonstrated that inducibility of ventricular arrhythmias was a reliable marker in patients with and without VF/SCD,[2,4] although Priori et al[3] did not find any significant difference in the analysis of all patients. A spontaneous type 1 ECG was also indicated as a reliable marker of poor prognosis by Brugada et al[4] in the analysis of patients without VF/SCD and by Eckardt et al[5] in all patients.[5] However, we could not find any reliability in these markers (Figures 3 and 5). Inducibility of ventricular arrhythmias was not a significant predictor even if it was evaluated by programmed pacing only from the RV apex (type 1 group: HR, 1.9 [95% CI, 0.7 to 5.2], P=0.18; all probands: HR, 1.5 [95% CI, 0.6 to 4.1], P=0.34, by univariate analysis).

In contrast, a family history of SCD occurring at age of <45 years is an independent risk factor of a poor prognosis in probands of any groups irrespective of their ECG type (type 1 or non–type 1) or symptoms (with VF or without VF). This was probably caused by a smaller proportion of probands with a family history of SCD as compared with previous studies[2–5] A family history was not found to be a marker in studies that enrolled many patients with SCD or a family history of Brugada syndrome. These results indicate that we should evaluate risks for arrhythmic events cautiously in studies with a significant number of family members.

Early repolarization pattern in the inferolateral leads was another indicator of poor prognosis, although Letsas et al[17] did not find any association with arrhythmic events in the data collected from 3 European centers, which also included ≈30% of patients with a family history of SCD. The reason for the poor outcome in probands with early repolarization in this study is not clear. However, it is conceivable that the combination of precordial Brugada-pattern ST-elevation with inferolateral early repolarization may represent electric heterogeneity in extensive regions of ventricles, which can result in lethal ventricular arrhythmias.

Study Limitations

In this study, premature ventricular electric stimulation was given until refractoriness was reached. The minimal

coupling interval of extrastimuli was not constant between participating hospitals and was sometimes shortened to <200 ms to induce ventricular arrhythmias.

We did not show the results of genetic analysis in this report, although more than half of the patients underwent genetic screening. Detailed results will be presented in a future report. So far, no positive relationship between genetic findings and patient outcomes has been found.[3,19]

We did not record ECGs at the higher intercostals spaces systematically except for probands with cardiac events, because the importance of "high-recording" became apparent in the course of this study.[6] Therefore, some patients of the non–type 1 group may have shown type 1 ST-elevation at the higher precordial positions.

Conclusions

This study described the long-term prognosis of probands with noncoved (non–type 1) Brugada-pattern ECG compared with type 1 ECG. The annual incidence of fatal arrhythmic events was similar between the 2 groups, which reached 10.6% in probands with non–type 1 ECG and a prior episode of VF. A family history of SCD occurring at age of <45 years and the presence of early repolarization were indicators of poor outcome although VF inducibility and a spontaneous type 1 ST-elevation were not reliable indicators in this prospective study including only probands.

Appendix

The following investigators and institutions participated in this study: A. Hukui, Yamagata University, Yamagata; M. Hiraoka, Tokyo Dental and Medical University, Tokyo; S. Takata, Kanazawa University, Kanazawa; H. Sakurada, Hiroo Metropolitan Hospital, Tokyo; Y. Eki, Ibaragi-higashi National Hospital, Tokai; Y. Sasaki, Nagano National Hospital, Ueda; Y. Tomita, Nagoya Medical Center, Nagoya; U. Shintani, Mie-chuo Medical Center, Tsu; T. Hashizume, Minami-Wakayama Medical Center, Tanabe; Y. Fujimoto, Okayama Medical Center, Okayama; W. Matsuura, Higashihiroshima Medical Center, Higashihiroshima; K. Sakabe, Zentuuji National Hospital, Zentuuji; and I. Matsuoka, Kagoshima Medical Center, Kagoshima, Japan.

Sources of Funding

This work was supported by a research grant for cardiovascular diseases (13A-1, 16C-3) from the Ministry of Health, Labor, and Welfare of Japan.

Disclosures

None.

References

1. Brugada P, Brugada J. Right bundle branch block, persistent ST segment elevation and sudden cardiac death: a distinct clinical and electrocardiographic syndrome: a multicenter report. *J Am Coll Cardiol.* 1992;20:1391–1396.
2. Brugada J, Brugada R, Antzelevitch C, Towbin J, Nademanee K, Brugada P. Long-term follow-up of individuals with the electrocardiographic pattern of right bundle-branch block and ST-segment elevation in precordial leads V1 to V3. *Circulation.* 2002;105:73–78.
3. Priori SG, Napolitano C, Gasparini M, Pappone C, Della Bella P, Giordano U, Bloise R, Giustetto C, De Nardis R, Grillo M, Ronchetti E, Faggiano G, Nastoli J. Natural history of Brugada syndrome: insights for risk stratification and management. *Circulation.* 2002;105:1342–1347.
4. Brugada J, Brugada R, Brugada P. Determinants of sudden cardiac death in individuals with the electrocardiographic pattern of Brugada syndrome and no previous cardiac arrest. *Circulation.* 2003;108:3092–3096.
5. Eckardt L, Probst V, Smits JP, Bahr ES, Wolpert C, Schimpf R, Wichter T, Boisseau P, Heinecke A, Breithardt G, Borggrefe M, LeMarec H, Bocker D, Wilde AA. Long-term prognosis of individuals with right precordial ST-segment-elevation Brugada syndrome. *Circulation.* 2005;111:257–263.
6. Shimizu W, Matsuo K, Takagi M, Tanabe Y, Aiba T, Taguchi A, Suyama K, Kurita T, Aihara N, Kamakura S. Body surface distribution and response to drugs of ST segment elevation in Brugada syndrome: clinical implication of eighty-seven-lead body surface potential mapping and its application to twelve-lead electrocardiograms. *J Cardiovasc Electrophysiol.* 2000;11:396–404.
7. Wilde AA, Antzelevitch C, Borggrefe M, Brugada J, Brugada R, Brugada P, Corrado D, Hauer RN, Kass RS, Nademanee K, Priori SG, Towbin JA; Study Group on the Molecular Basis of Arrhythmias of the European Society of Cardiology. Proposed diagnostic criteria for the Brugada syndrome: consensus report. *Circulation.* 2002;106:2514–2519.
8. Antzelevitch C, Brugada P, Borggrefe M, Brugada J, Brugada R, Corrado D, Gussak I, LeMarec H, Nademanee K, Perez Riera AR, Shimizu W, Schulze-Bahr E, Tan H, Wilde AA. Brugada syndrome: report of the second consensus conference; endorsed by the Heart Rhythm Society and the European Heart Rhythm Association. *Circulation.* 2005;111:659–670.
9. Haïssaguerre M, Derval N, Sacher F, Jesel L, Deisenhofer I, de Roy L, Pasquié JL, Nogami A, Babuty D, Yli-Mayry S, De Chillou C, Scanu P, Mabo P, Matsuo S, Probst V, Le Scouarnec S, Defaye P, Schlaepfer J, Rostock T, Lacroix D, Lamaison D, Lavergne T, Aizawa Y, Englund A, Anselme F, O'Neill M, Hocini M, Lim KT, Knecht S, Veenhuyzen GD, Bordachar P, Chauvin M, Jais P, Coureau G, Chene G, Klein GJ, Clémenty J. Sudden cardiac arrest associated with early repolarization. *N Engl J Med.* 2008;358:2016–2023.
10. Hattori Y, Inomata N. Modes of the Na channel blocking action of pilsicainide, a new antiarrhythmic agent, in cardiac cell. *Japan J Pharmacol.* 1992;58:365–373.
11. Morita H, Morita ST, Nagase S, Banba K, Nishii N, Tani Y, Watanabe A, Nakamura K, Kusano KF, Emori T, Matsubara H, Hina K, Kita T, Ohe T. Ventricular arrhythmia induced by sodium channel blocker in patients with Brugada syndrome. *J Am Coll Cardiol.* 2003;42:1624–1631.
12. Letsas KP, Efremidis M, Gavielatos G, Filippatos GS, Sideris A, Kardaras F. Neurally mediated susceptibility in individuals with Brugada-type ECG pattern. *Pacing Clin Electrophysiol.* 2008;31:418–421.
13. Nademanee K, Veerakul G, Nimmannit S, Nimmannit S, Chaowakul V, Bhuripanyo K, Likittanasombat K, Tunsanga K, Kuasirikul S, Malasit P, Tansupasawadikul S, Tatsanavivat P. Arrhythmogenic marker for the sudden unexplained death syndrome in Thai men. *Circulation.* 1997;96:2595–2600.
14. Bezzina CR, Shimizu W, Yang P, Koopmann TT, Tanck MWT, Miyamoto Y, Kamakura S, Roden DM, Wilde AA. Common sodium channel promoter haplotype in Asian subjects underlies variability in cardiac conduction. *Circulation.* 2006;113:338–344.
15. Sacher F, Probst V, Iesaka Y, Jacon P, Laborderie J, Mizon-Gérard F, Mabo P, Reuter S, Lamaison D, Takahashi Y, O'Neill MD, Garrigue S, Pierre B, Jaïs P, Pasquié JL, Hocini M, Salvador-Mazenq M, Nogami A, Amiel A, Defaye P, Bordachar P, Boveda S, Maury P, Klug D, Babuty D, Haïssaguerre M, Mansourati J, Clémenty J, Le Marec H. Outcome after implantation of a cardioverter-defibrillator in patients with Brugada syndrome: a multicenter study. *Circulation.* 2006;114:2317–2324.
16. Miyamoto K, Yokokawa M, Tanaka K, Nagai T, Okamura H, Noda T, Satomi K, Suyama K, Kurita T, Aihara N, Kamakura S, Shimizu W. Diagnostic and prognostic value of a type 1 Brugada electrocardiogram at higher (third or second) V1 to V2 recording in men with Brugada syndrome. *Am J Cardiol.* 2007;99:53–57.
17. Letsas KP, Sacher F, Probst V, Weber R, Knecht S, Kalusche D, Haïssaguerre M, Arentz T. Prevalence of early repolarization pattern in inferolateral leads in patients with Brugada syndrome. *Heart Rhythm.* 2008;5:1685–1689.
18. Haïssaguerre M, Sacher F, Nogami A, Komiya N, Bernard A, Probst V, Yli-Mayry S, Defaye P, Aizawa Y, Frank R, Mantovan R, Cappato R, Wolpert C, Leenhardt A, de Roy L, Heidbuchel H, Deisenhofer I, Arentz T, Pasquié JL, Weerasooriya R, Hocini M, Jais P, Derval N, Bordachar P,

Clémenty J. Characteristics of recurrent ventricular fibrillation associated with inferolateral early repolarization: role of drug therapy. *J Am Coll Cardiol.* 2009;53:612–619.
19. Kusano KF, Taniyama M, Nakamura K, Miura D, Banba K, Nagase S, Morita H, Nishii N, Watanabe A, Tada T, Murakami M, Miyaji K, Hiramatsu S, Nakagawa K, Tanaka M, Miura A, Kimura H, Fuke S, Sumita W, Sakuragi S, Urakawa S, Iwasaki J, Ohe T. Atrial fibrillation in patients with Brugada syndrome relationships of gene mutation, electrophysiology, and clinical backgrounds. *J Am Coll Cardiol.* 2008;51:1176–1180.

CLINICAL PERSPECTIVE

The prognosis of patients with saddleback or noncoved type (non–type 1) ST-elevation in Brugada syndrome is unknown. We compared the long-term prognosis of 85 probands with non–type 1 ECG with 245 probands with coved (type 1) Brugada-pattern ECG prospectively. The absence of type 1 ECG was confirmed by drug provocation test and multiple recordings. Clinical profiles and outcomes did not differ between the non–type 1 and type 1 groups. The annual rate of fatal arrhythmic events was very low in asymptomatic probands and those with syncope but was higher in probands with ventricular fibrillation. A family history of sudden cardiac death at age <45 years and the presence of inferolateral early repolarization were indicators of poor prognosis, although ventricular fibrillation inducibility and a spontaneous type 1 ST-elevation were not reliable parameters in this prospective study including only probands.

Latent Genetic Backgrounds and Molecular Pathogenesis in Drug-Induced Long-QT Syndrome

Hideki Itoh, MD; Tomoko Sakaguchi, MD; Wei-Guang Ding, MD; Eiichi Watanabe, MD; Ichiro Watanabe, MD; Yukiko Nishio, MD; Takeru Makiyama, MD; Seiko Ohno, MD; Masaharu Akao, MD; Yukei Higashi, MD; Naoko Zenda, MD; Tomoki Kubota, MD; Chikara Mori, MD; Katsunori Okajima, MD; Tetsuya Haruna, MD; Akashi Miyamoto, MD; Mihoko Kawamura, MD; Katsuya Ishida, MD; Iori Nagaoka, MD; Yuko Oka, MD; Yuko Nakazawa, MD; Takenori Yao, MD; Hikari Jo, MD; Yoshihisa Sugimoto, MD; Takashi Ashihara, MD; Hideki Hayashi, MD; Makoto Ito, MD; Keiji Imoto, MD; Hiroshi Matsuura, MD; Minoru Horie, MD

Background—Drugs with I_{Kr}-blocking action cause secondary long-QT syndrome. Several cases have been associated with mutations of genes coding cardiac ion channels, but their frequency among patients affected by drug-induced long-QT syndrome (dLQTS) and the resultant molecular effects remain unknown.

Methods and Results—Genetic testing was carried out for long-QT syndrome–related genes in 20 subjects with dLQTS and 176 subjects with congenital long-QT syndrome (cLQTS); electrophysiological characteristics of dLQTS-associated mutations were analyzed using a heterologous expression system with Chinese hamster ovary cells together with a computer simulation model. The positive mutation rate in dLQTS was similar to cLQTS (dLQTS versus cLQTS, 8 of 20 [40%] versus 91 of 176 [52%] subjects, $P=0.32$). The incidence of mutations was higher in patients with torsades de pointes induced by nonantiarrhythmic drugs than by antiarrhythmic drugs (antiarrhythmic versus others, 3 of 14 [21%] versus 5 of 6 [83%] subjects, $P<0.05$). When reconstituted in Chinese hamster ovary cells, *KCNQ1* and *KCNH2* mutant channels showed complex gating defects without dominant negative effects or a relatively mild decreased current density. Drug sensitivity for mutant channels was similar to that of the wild-type channel. With the Luo-Rudy simulation model of action potentials, action potential durations of most mutant channels were between those of wild-type and cLQTS.

Conclusions—dLQTS had a similar positive mutation rate compared with cLQTS, whereas the functional changes of these mutations identified in dLQTS were mild. When I_{Kr}-blocking agents produce excessive QT prolongation (dLQTS), the underlying genetic background of the dLQTS subject should also be taken into consideration, as would be the case with cLQTS; dLQTS can be regarded as a latent form of long-QT syndrome. **(*Circ Arrhythmia Electrophysiol.* 2009;2:511-523.)**

Key Words: long-QT syndrome ■ secondary ■ drug ■ electrophysiology ■ ion channel

Congenital long-QT syndrome (cLQTS) is characterized by abnormally prolonged ventricular repolarization and familial inheritance, leading to polymorphic ventricular tachycardia (torsades de pointes [TdP]), causing sudden cardiac death.[1,2] In contrast, secondary long-QT syndrome can be induced by a variety of commercially available drugs, including antiarrhythmic drugs, antihistamines, antibiotics, and major tranquilizers.[3] In patients with drug-induced long-QT syndrome (dLQTS), after a washout period of the culprit drugs, the QT interval usually returns to within normal range. Genetic factors may underlie the susceptibility to drug-induced serious adverse reactions such as a long QT

Clinical Perspective on p 523

Received February 29, 2008; accepted July 6, 2009.

From the Department of Cardiovascular and Respiratory Medicine (H.I., T.S., A.M., M.K., K.I., I.N., Y.O., Y.N., T.Y., H.J., Y.S., T.A., H.H., M.I., M.H.) and the Department of Physiology (W.-G.D., H.M.), Shiga University of Medical Science, Shiga, Japan; the Department of Laboratory Medicine (E.W.), Fujita Health University School of Medicine, Toyoake, Japan; the Division of Cardiology (I.W.), Department of Medicine, Nihon University School of Medicine, Tokyo, Japan; the Department of Cardiovascular Medicine (Y.N., T.M., S.O., M.A.), Kyoto University Graduate School of Medicine, Kyoto, Japan; the Cardiovascular Division (Y.H., N.Z.), Showa University Fujigaoka Hospital, Yokohama, Japan; the Division of Cardiology (T.K.), Gifu University Graduate School of Medicine, Gifu, Japan; the Division of Cardiology (C.M.), Department of Internal Medicine, Jikei University School of Medicine, Daisan Hospital, Tokyo, Japan; the Department of Cardiology (K.O.), Hyogo Brain and Heart Center, Himeji, Japan; the Department of Cardiology (T.H.), Kitano Hospital, Osaka, Japan; and the Department of Information Physiology (K.I.), National Institute for Physiological Sciences, Okazaki, Japan.

The online-only Data Supplement is available at http://circep.ahajournals.org/cgi/content/full/CIRCEP.109.862649/DC1.

Correspondence to Minoru Horie, MD, Department of Cardiovascular and Respiratory Medicine, Shiga University of Medical Science, Seta-Tsukinowa, Otsu, Shiga, Japan 520-2192. E-mail horie@belle.shiga-med.ac.jp

Circ Arrhythmia Electrophysiol **is available at http://circep.ahajournals.org** **DOI: 10.1161/CIRCEP.109.862649**

interval and TdP. Sesti et al[4] demonstrated that a polymorphism of the *KCNE2* gene (T8A) is present in 1.6% of the population and is associated with drug-induced TdP related to quinidine and to sulfamethoxazole/trimethoprim administration. We have also previously reported that a mutant *SCN5A* channel (L1825P), found in an elderly woman with cisapride-induced TdP, appeared to have unique electrophysiological characteristics with both loss and gain of functions for the cardiac sodium current.[5] In addition, there have been several case reports with long-QT syndrome–associated gene mutations in dLQTS.[6–10] The accurate prevalence of long-QT syndrome–related gene mutations in a larger dLQTS cohort, however, remains unknown, and the relationship between genotypes and cellular electrophysiology has not been fully examined. The present study therefore aimed to survey mutations in long-QT syndrome–related genes responsible for dLQTS in 20 patients who had been referred to our institutes consecutively over the past 11 years and analyze the functional effects induced by these mutations.

Methods

Subjects

Blood samples of 305 subjects with long-QT syndrome, comprising 196 long-QT syndrome probands and 109 family members were referred to Kyoto University Graduate School of Medicine and Shiga University of Medical Sciences from March 1996 to January 2006 for genetic analysis. A diagnosis of dLQTS was made in those subjects who had not previously been diagnosed with long-QT syndrome and who only developed typical ECG features of QT prolongation after administration of culprit drugs. A diagnosis of cLQTS was made in those subjects with clinical phenotypes of long-QT syndrome, but without the involvement of secondary factors (eg, drugs, hypokalemia, or bradycardia). Among the subjects, 20 probands had drug-induced cardiac events (10.2% of long-QT syndrome probands). Their clinical information was collected, including family history of sudden death age 30 years or younger and long-QT syndrome members, previous syncope, ECGs, and serum electrolyte levels at the time of cardiac events. TdP was defined as either nonsustained or sustained ventricular tachycardia showing variation in the electronic polarity of the QRS complex and a "short-long-short" initiating sequence.[11] Written informed consent was obtained from all subjects in accordance with the guidelines approved by our institutional review board. QT intervals were measured in lead II or V_5, using the Bazett formula,[12] before and after allowing sufficient time for the complete washout of drugs.

Schwartz scores[13] were calculated in all probands. A Schwartz score $\geqq 4$ points indicates that long-QT syndrome is definitely present, a score of 2 or 3 points indicates there is a strong possibility that long-QT syndrome is present, whereas a score $\leqq 1$ point indicates a low probability of long-QT syndrome, respectively.[13]

Mutation Analysis

The protocol for genetic analysis was approved by and performed under the guidelines of the Institutional Ethics Committee at Shiga University of Medical Science. Genomic DNA was isolated from peripheral white blood cells using conventional methods. Genetic screening was performed for *KCNQ1, KCNH2, SCN5A, KCNE1, KCNE2,* and *KCNJ2,* using polymerase chain reaction/single-strand conformational polymorphism (PCR-DHPLC, WAVE system, Transgenomic Inc, Omaha, Neb) analysis.[14,15] For the abnormal DHPLC patterns, we determined the DNA sequences on both strands with an automated sequencer (PRISM 3130 Sequencer, Perkin Elmer, Calif).

Expression Plasmids

The expression plasmids pIRES2-EGFP/*KCNQ1*(wild type[WT]/*KCNQ1*) and pRc-CMV/*KCNH2* (wild-type [WT]/*KCNH2*) were kindly provided by Dr J. Barhanin (UMR 6097 CNRS and Université de Nice Sophia Antipolis, Valbonne, France) and Dr M. Sanguinetti (University of Utah, Salt Lake City, Utah), respectively. The mutations were introduced using overlap PCR. The mutant plasmids were constructed by substituting the 857-bp *Xho*I-*Bgl*II for R231C and R243H mutants, 287-bp *Eag*I-*Bst*EII for the D342V mutant, 794-bp *Bst*EII-*Bgl*II for the H492Y mutant, or 392-bp *Bgl*II-*Sph*I fragments for S706F and M756V mutants, respectively, for the corresponding fragments of WT/*KCNQ1* or WT/*KCNH2*.

Cell Transfection

Functional potassium channels were expressed transiently in Chinese hamster ovary (CHO) cells by transfecting the same amount of α subunit plasmids (1 μg/mL *KCNQ1* cDNA or 2 μg/mL *KCNH2* cDNA). For the analysis of I_{Ks} currents, the same amount of pIRES/CD8-*KCNE1* was coexpressed. Cells were trypsinized, diluted with Dulbecco Modified Eagle's Medium (DMEM, Nacalai Tesque, Kyoto, Japan) supplemented with 10% fetal bovine serum, 30 U/mL penicillin, and 30 μg/mL streptomycin. The DMEM used for cell culture dishes was changed to OptiMEM (Invitrogen, Carlsbad, Calif) for transfection, and, after the addition of 10 μL lipofectamine (Invitrogen) and cDNA, the cells were incubated at 37°C for 3 hours, unless otherwise described. OptiMEM was then replaced by DMEM and the cells were subjected to electrophysiological measurements 48 to 72 hours after transfection. Cells expressing the potassium channels were selected through detection of green fluorescent protein and by decoration with anti-CD8 antibody-coated beads.

Electrophysiology

Whole-cell patch-clamp recordings were made at 37°C, using an EPC-8 patch-clamp amplifier (HEKA, Lambrecht, Germany) with pipettes filled with (in mM): 70 aspartate, 70 KOH, 40 KCl, 10 KH_2PO_4, 1 $MgSO_4$, 3 Na_2-ATP, 0.1 Li_2-GTP, 5 HEPES, and 5 EGTA (pH 7.3 with 1N KOH), with a resistance of 2.0 to 4.0 mol/LΩ. The external superfusate contained (in mM): NaCl 140, KCl 5.4, $MgCl_2$ 0.5, $CaCl_2$ 1.8, NaH_2PO_4 0.33, glucose 5.5, and HEPES 5 (pH 7.4 with NaOH). Data were filtered at 2 kHz. Data acquisition was performed using PatchMaster acquisition software (HEKA). The holding potential was set at −80 mV. Current densities (pA/pF) were calculated for each cell studied, by normalizing peak tail current amplitude to cell capacitance. Current-voltage relations were fitted with the Boltzmann function:

$$I/I_{max}=1/(1+\exp((V_{1/2}-Vm)/k))$$

where $V_{1/2}$ indicates the potential at which the activation or inactivation is half-maximal, Vm the test potential, and k the slope factor.

Drug sensitivities were examined by various concentrations for erythromycin, disopyramide, and pirmenol (gift from Pfizer Inc, Groton, Conn). Depolarizing pulses were applied every 15 seconds and peak tail currents at −60 mV after +20 mV test potential were recorded in the absence or presence of various concentrations of agent. Percent inhibition was calculated by dividing the peak amplitude in the presence of drug by control. Drug concentration-inhibition relations were fitted to the Hill equation;

$$\text{Fractional drug inhibition}=1/(1+([IC_{50}]/[\text{drug}])^n)$$

where IC_{50} is the amount of drug necessary to produce the half-maximal inhibition of I_{Kr} tail currents, and n is the Hill coefficient for the fit.

Computer Simulation

The dynamic Luo-Rudy model (Clancy and Rudy 2001 model) of a ventricular cell was used, with recent modifications and action potentials were simulated using a previously reported model.[16] The ratio of I_{Kr} and I_{Ks} conductance of M cell layer was set at 23:7. Based

on the experimental data of voltage-clamp recordings of *KCNQ1* and *KCNH2* channels heterologously expressed in CHO cells, we constructed Markov or Hodgkin-Huxley models for simulated mutant channels as compared with mutants associated with cLQTS (see supplemental data 1). To make the mutant channel models, we decreased the conductance of each channel as appropriate for the decreased current density and looked for adequate changes for mutant channels by changing each coefficient value, in turn, for gating states associated with impaired gating defects. The simulation for voltage-clamp experiments was calculated using the 4th-order Runge-Kutta method with a fixed-time step of 0.020 ms. The simulation programs (see supplemental data 1) were coded in C++ and implemented for personal computers.

Statistical Analysis

Experimental data are expressed as mean±SE and other clinical data as mean±SD, and the statistical comparisons were made using the unpaired Student *t* test. Differences in the positive mutation rate between 2 groups were analyzed by χ^2 and Fisher exact probability test. Statistical significance was considered as $P<0.05$.

Results

Molecular Genetics of dLQTS

Table 1 summarizes the clinical characteristics of 20 subjects with dLQTS (14 women and 6 men; mean age, 65±16 years). Nineteen subjects had TdP with marked QT prolongation, and 1 had syncope without documented TdP after taking 1 of the drugs listed in Table 1. The average QT_c interval before taking drugs, available for 15 subjects, was 446±29 ms. The QT_c interval was significantly prolonged to 616±91 ms after taking 1 of the culprit drugs (versus QT_c interval before taking drugs, $P<0.001$) and significantly shortened to 441±33 ms after washout of drugs (versus QT_c interval after taking drugs, $P<0.001$). However, in 3 patients (cases 8, 13, and 18 in Table 1) a prolonged QT interval of over 480 ms was maintained after washout. The average R-R interval immediately before TdP was 1.2±0.4 seconds, and the average serum potassium level after TdP was 3.9±0.6 mEq/mL. In the majority of subjects (n=14, 70%), dLQTS was induced by antiarrhythmic drugs (disopyramide, pirmenol, cibenzoline, procainamide, and aprindine in 8, 3, 1, 1, and 1 subjects, respectively; cases 1 to 14); the remaining cases were induced by antihistamines, antibiotics, psychiatric, or miscellaneous drugs (cases 15 to 20 in Table 1). None had a family history of long-QT syndrome, whereas 3 subjects (cases 4, 14, and 20) had unexplained syncope and another subject (case 17) had a family member with sudden cardiac death. During a mean follow-up period of 52±44 months after discontinuing drugs, 1 subject without any gene mutations (case 9) had recurrent ventricular fibrillation. Compared with cLQTS, the age at first cardiac event in subjects diagnosed with dLQTS was significantly older (dLQTS versus cLQTS; 65±16 versus 19±18 years, $P<0.001$). No subject in the dLQTS group had a family member with long-QT syndrome (dLQTS versus cLQTS; 0% versus 24% subjects, $P<0.01$). The QT_c interval in dLQTS subjects was significantly shorter than in cLQTS subjects (dLQTS versus cLQTS; 446±29 versus 507±71 ms, $P<0.001$); the Schwartz score was significantly lower in dLQTS than in cLQTS (dLQTS versus cLQTS; 0.9±1.4 versus 4.1±2.1, $P<0.001$).

In 8 (40%) dLQTS subjects, the genetic analysis identified 8 mutations in LQTS-related genes; 2 *KCNQ1*, 5 *KCNH2*, and 1 *SCN5A* (Table 1). These variants were not observed in the control subjects (220 chromosomes from non-cLQTS and non-dLQTS subjects), suggesting that they represented disease-related mutations. The 91 cLQTS patients also had gene mutations such as 33 *KCNQ1*, 36 *KCNH2*, 12 *SCN5A*, 2 *KCNE2*, and 8 compound mutations, and the positive mutation rate was similar between dLQTS and cLQTS subjects (8 of 20 [40%] versus 91 of 176 [52%] subjects, respectively, $P=0.32$, Figure 1A). These mutations were found in only 3 of 14 (21%) subjects with TdP induced by antiarrhythmic drugs. In contrast, 5 of 6 subjects with TdP induced by nonantiarrhythmic drugs had gene mutations (83%; versus patients with TdP induced by antiarrhythmic drugs, $P<0.05$) (Figure 1B). Seven of the 8 mutations were located in the nonpore regions (red circles in Figure 1C), except for the A614V-*KCNH2* mutation in a case of hydroxyzine-induced TdP.[17] The green circles in Figure 1C indicate the location of 8 mutations previously reported in dLQTS.[5-10]

Clinical Characteristics of Genotyped dLQTS Subjects

Detailed subject characteristics are presented in Table 1 and the supplemental data 2. Case 2 (M756V/*KCNH2*) was a 63-year-old man who was admitted with syncope after taking pirmenol (300 mg/d). Case 4 (H492Y/*KCNH2*) was a 52-year-old woman who had syncope while taking disopyramide (300 mg/d). She had previously had 1 episode of unexplained syncope. Case 14 (R243H/*KCNQ1*) was a 52-year-old woman who had repetitive syncope after taking aprindine (60 mg/d). Case 15 (S706F/*KCNH2*) was a 21-year-old woman who complained of sudden onset of palpitations and dyspnea after taking amphetamine and methamphetamine. An *SCN5A* mutation (L1825P/*SCN5A*) (case 16), has been reported previously[5]; this concerned a 70-year-old woman who had TdP and prolongation of the QT interval after taking cisapride (5 mg/d) and pirmenol (200 mg/d). Case 17 (D342V/*KCNH2*) was a 70-year-old woman who had repetitive syncope due to erythromycin intake (1200 mg/d). This subject had a 24-year-old sister who had died suddenly, but it is not unknown if her sister had suffered from LQTS. Case 18 (R231C/*KCNQ1*) was a 72-year-old woman who had presyncope while taking probucol (250 mg/d). Case 20 concerned a 34-year-old woman (A614V/*KCNH2* according to Table 1) who had syncope and QT prolongation induced by hydroxyzine (3 mg/d).[17] None of the 20 subjects in the study had structural heart disease or a family history of documented LQTS. In genotyped families, a genetic test for 5 members revealed 1 R243H/*KCNQ1* mutation carrier. This carrier had no syncope and a normal QT interval (QT_c, 400 ms). The Schwartz scores in the 8 subjects with mutations were 1.0±1.5 points (range, 0 to 4 points). Thus, among the genotyped dLQTS subjects in this current study, there was only a low or moderate possibility of LQTS being present, both before taking the drugs or after their withdrawal.

Table 1. Clinical Characteristics and Gene Mutations of Probands With Drug-Induced Arrhythmic Events

No.	Age, y	Sex	Drug Types	Culprit Drugs, Dose/d	Cardiac Events	Previous Syncope/LQTS Members	QTc, ms			Serum K, mEq/l, After TdP	R-R Interval Before TdP, s	Nucleotide Change	Mutation/Gene
							Before Taking Drugs	After Events	After Washout of Drugs				
1	68	M	Antiarrhythmic drug	Disopyramide, 300 mg	TdP	−/−	421	609	425	4.4	0.7		
2	63	M	Antiarrhythmic drug	Pirmenol, 150 mg	TdP	−/−	453	632	Normal	NA	1.1	a2266g	M756V/KCNH2
3	81	F	Antiarrhythmic drug	Disopyramide, 300 mg	TdP	−/−	447	563	456	2.8	1.3		
4	52	F	Antiarrhythmic drug	Disopyramide, 300 mg	TdP	+/−	495	585	447	3.2	1.1	c1474t	H492Y/KCNH2
5	74	M	Antiarrhythmic drug	Disopyramide, 300 mg	TdP	−/−	383	553	370	4.0	0.9		
6	86	F	Antiarrhythmic drug	Cibenzoline, 100 mg	TdP	−/−	NA	620	430	4.3	1.4		
7	56	F	Antiarrhythmic drug	Disopyramide, 300 mg	TdP	−/−	446	577	383	NA	1.2		
8	79	F	Antiarrhythmic drug	Disopyramide, 300 mg	TdP	−/−	Kent (+)	597	495	NA	NA		
9	77	M	Antiarrhythmic drug	Pirmenol, 200 mg	TdP	−/−	450	538	449	4.3	2.1		
10	69	F	Antiarrhythmic drug	Disopyramide, 150 mg	TdP	−/−	421	557	403	4.1	NA		
11	67	F	Antiarrhythmic drug	Disopyramide, 50 mg*	TdP	−/−	464	506	435	NA	1.4		
12	62	M	Antiarrhythmic drug	Pirmenol, 200 mg	TdP	−/−	430	484	424	4.1	1.0		
13	61	M	Antiarrhythmic drug	Procainamide, 200 mg*	TdP	−/−	487	705	496	4.9	NA		
14	52	F	Antiarrhythmic drug	Aprindine, 60 mg	TdP	+/−	NA	857	469	4.2	TdP on adm.	g728a	R243H/KCNQ1
15	21	F	Nonantiarrhythmic drug	3,4-Methylenedioxymethamphetamine, 10 tabs	TdP	−/−	426	600	450	3.4	TdP on adm.	c2117t	S706F/KCNH2
16	70	F	Nonantiarrhythmic drug	Cisapride, 5 mg	TdP	−/−	435	731	417	3.8	1.5	t5474c	L1825P/SCN5A
17	70	F	Nonantiarrhythmic drug	Erythromycin, 1200 mg	TdP	−/−	454	776	440 (AF)	3.9	0.9	a1025t	D342V/KCNH2
18	72	F	Nonantiarrhythmic drug	Probucol, 250 mg	TdP	−/−	480 (AF)	754	495 (AF)	3.2	1.0	c691t	R231C/KCNQ1
19	77	F	Nonantiarrhythmic drug	Haloperidol, 5 mg	TdP	−/−	NA	574	447	4.6	4.6		
20	34	F	Nonantiarrhythmic drug	Hydroxydine, 3 mg	syncope	+/−	Untested	626	449	Untested	Untested	c1841t	D614V/KCNH2
Ave±SD	65±16						446±29	616±91	441±33	3.9±0.6	1.2±0.4		

M indicates male; F, female; NA, not available; AF, atrial fibrillation; Kent (+), type A Wolf-Parkinson-White syndrome; prolonged QT, ECG shows prolonged QT interval but unspecified QT interval; normal, normal QT interval but unspecified QT interval.

*Intravenous administration.

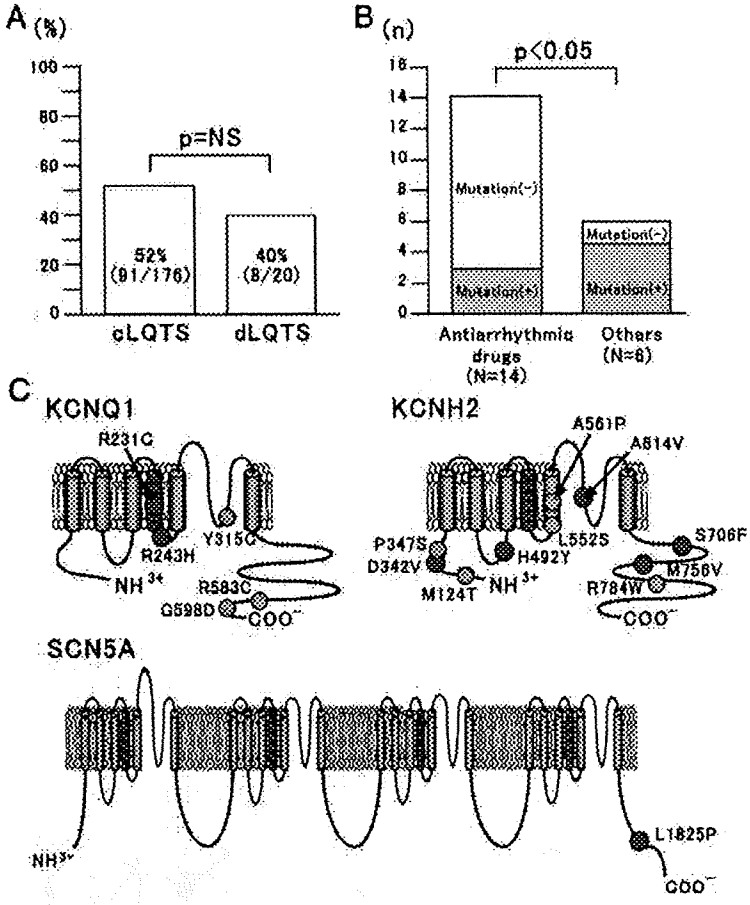

Figure 1. Molecular genetics of gene mutations in subjects with drug-induced long QT syndrome (LQTS). A, A pie graph showing the incidence of mutation carriers in our drug-induced LQTS cohort. B, Bar graph showing different mutation detection rates depending on culprit drugs. C, Schemes indicating the location associated with drug-induced LQTS. Red circles indicate the sites of mutations detected in this study; green circles indicate previously reported mutations.

Electrophysiological Characteristics of Mutations Associated With dLQTS

The biophysical effects of the respective *KCNQ1* and *KCNH2* mutations were analyzed using a heterologous expression system with the CHO cell line. The upper panel of Figure 2A shows representative current traces for WT and 2 mutant *KCNQ1* channels; the lower panel shows those recorded from cells cotransfected with WT and each mutant. On their own, both mutants displayed smaller currents compared with WT, whereas the R231C channel was a slightly open K^+ leak channel. Under heterozygous conditions, however, they displayed currents comparable to those of WT without dominant negative effects.

At the end of the depolarizing pulse to +40 mV, current densities were smaller than those of WT channels (77.0±10.6 pA/pF) in R231C/WT (39.6±11.9 pA/pF, $P<0.05$ versus WT) but not in R243H/WT (61.9±10.7 pA/pF) (Figure 2B). On the other hand, the R243H channels showed a significant positive shift of steady-state activation curve (Figure 2C). Half activation voltages ($V_{1/2}$) and k were −8.2±3.1 mV and 12.6±0.6 for WT, −12.8±3.6 mV and 13.6±1.3 for R231C/WT, 1.7±3.1 mV and 12.9±0.6 for R243H/WT, respectively ($V_{1/2}$: WT versus R243H/WT, $P<0.05$). Figure 2D shows representative families of current traces (left panel) and time constants (right panel) of deactivation in each channel. The time course of deactivating kinetics could be fitted by a single-exponential function. The R243H/WT channel had faster deactivation process over −60 mV, whereas this process in the R231C/WT channel was slower than WT under −90 mV.

Figure 3A shows representative families of current traces recorded during depolarizing pulses from CHO cells transfected with *KCNH2* cDNAs as indicated in the graph. The left column depicts current traces from cells transfected with each construct alone and the right column those recorded under heterozygous conditions except for the uppermost traces (WT 1 μg). When expressed alone, D342V was nonfunctional and 3 other mutations displayed functional channels. When coexpressed with WT, D342V showed weak dominant negative effects, whereas the other 3 channels showed nondominant negative effects. The functional outcome of the remaining mutation, A614V-*KCNH2*, [17] has recently been reported. Using an oocyte expression system, Nakajima et al[18] reported that the A614V channel showed loss of function in a dominant negative manner, and the results from the present study were almost identical (18% current density of WT).

Current densities at the end of a 2-second depolarization pulse were calculated in multiple cells and plotted as a function of test potential in Figure 3B. At the end of the depolarizing pulse to +20 mV, the densities were smaller than those of WT channels (36.2±6.8 pA/pF) in D342V/WT (18.7±4.5 pA/pF, $P<0.05$ versus WT) and S706F/WT (21.9±2.7 pA/pF, $P=0.055$ versus WT). Those in

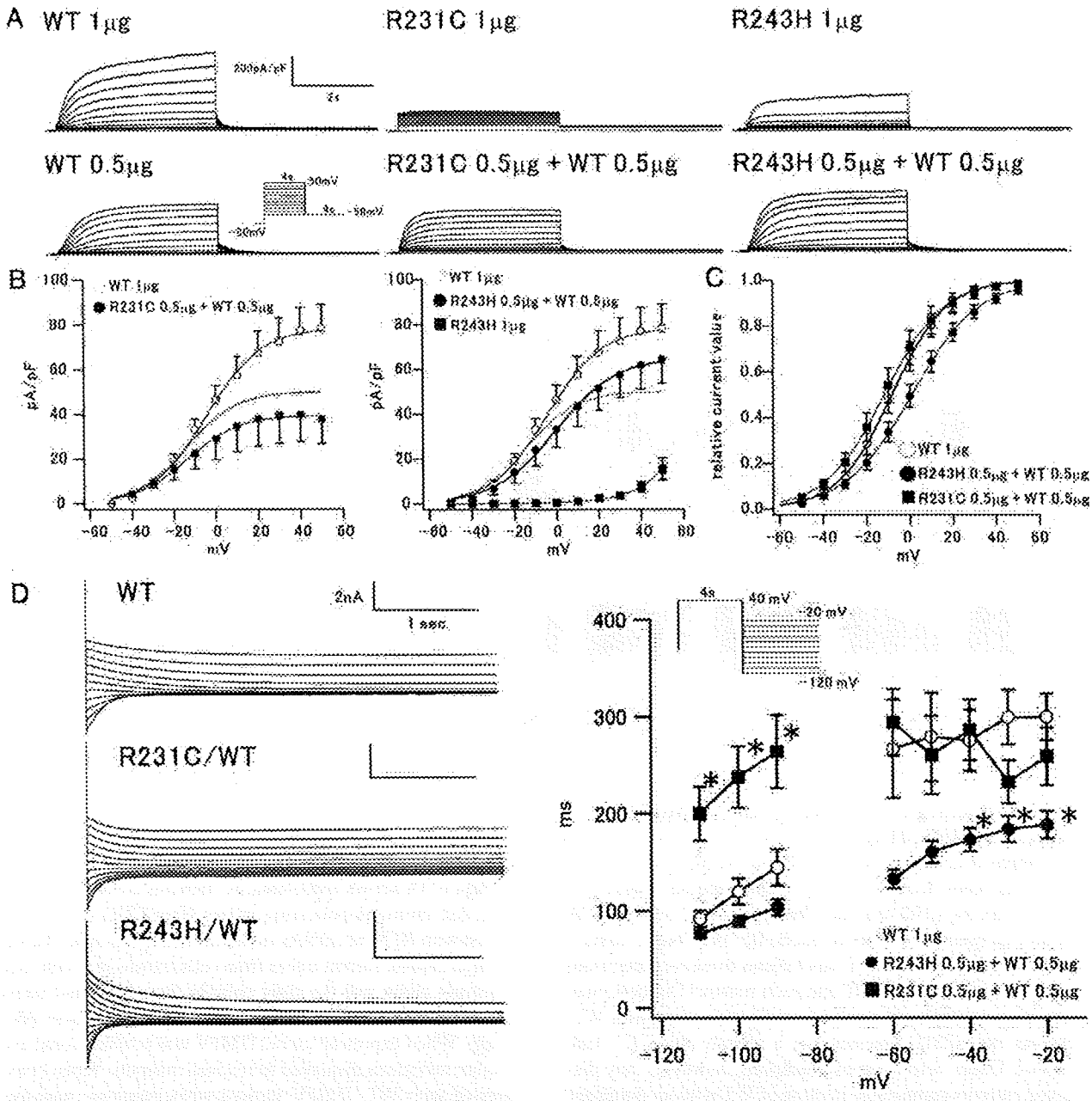

Figure 2. Mutations associated with nondominant negative effects of *KCNQ1* channels. A, Current traces reconstituted in CHO. Current amplitude was normalized by respective cell capacitance and was indicated as the current density. B, Current-voltage (I-V) relationships for amplitudes of steady-state currents at the end of 4-second depolarizing pulses. Currents were elicited by depolarizing pulses from a holding potential of −80 mV to test potential between −50 to +50 mV (with a 10-mV step increment), followed by repolarization to −50 mV to monitor tail current amplitude. The voltage-clamp protocol is shown in the inset. Open circles, WT (1 μg); filled squares, mutant (1 μg); filled circles, WT (0.5 μg) plus mutant (0.5 μg); and dotted lines, WT (0.5 μg). All data were recorded from 10 to 25 cells. C, Steady-state activation curves for WT and WT plus mutants. D, *KCNQ1* mutants modify deactivation time curse. Left column presents the time course of deactivation for each channel. Each inset illustrates scale bars of 2-nA and 1-second times. To examine the deactivation time course, a conditioning pulse to +40 mV for 4 seconds from a holding potential of −80 mV was followed by hyperpolarizing test pulses between −120 mV and −20 mV in 10-mV increments (inset in graph on right). Currents were not leak-subtracted. Deactivation time constants (tau) were measured by fitting deactivating currents during test pulses at each potential with a single exponential. *$P<0.05$ versus WT.

H492Y/WT and M756V/WT were also smaller than in the WT, but the difference did not reach statistical significance.

The mean peak amplitudes of tail currents at −60 mV on repolarization from various test potentials (2-second duration) plotted as a function of test potentials are displayed in Figure 3C. H492Y and M756V channels displayed amplitudes of peak tail currents similar to WT. For example, the peak tail current densities after a test pulse to +20 mV were 66.2±10.5 pA/pF for WT, 62.1±13.0 pA/pF for H492Y/WT, and 58.4±7.7 pA/pF for M756V/WT. On the other hand, the

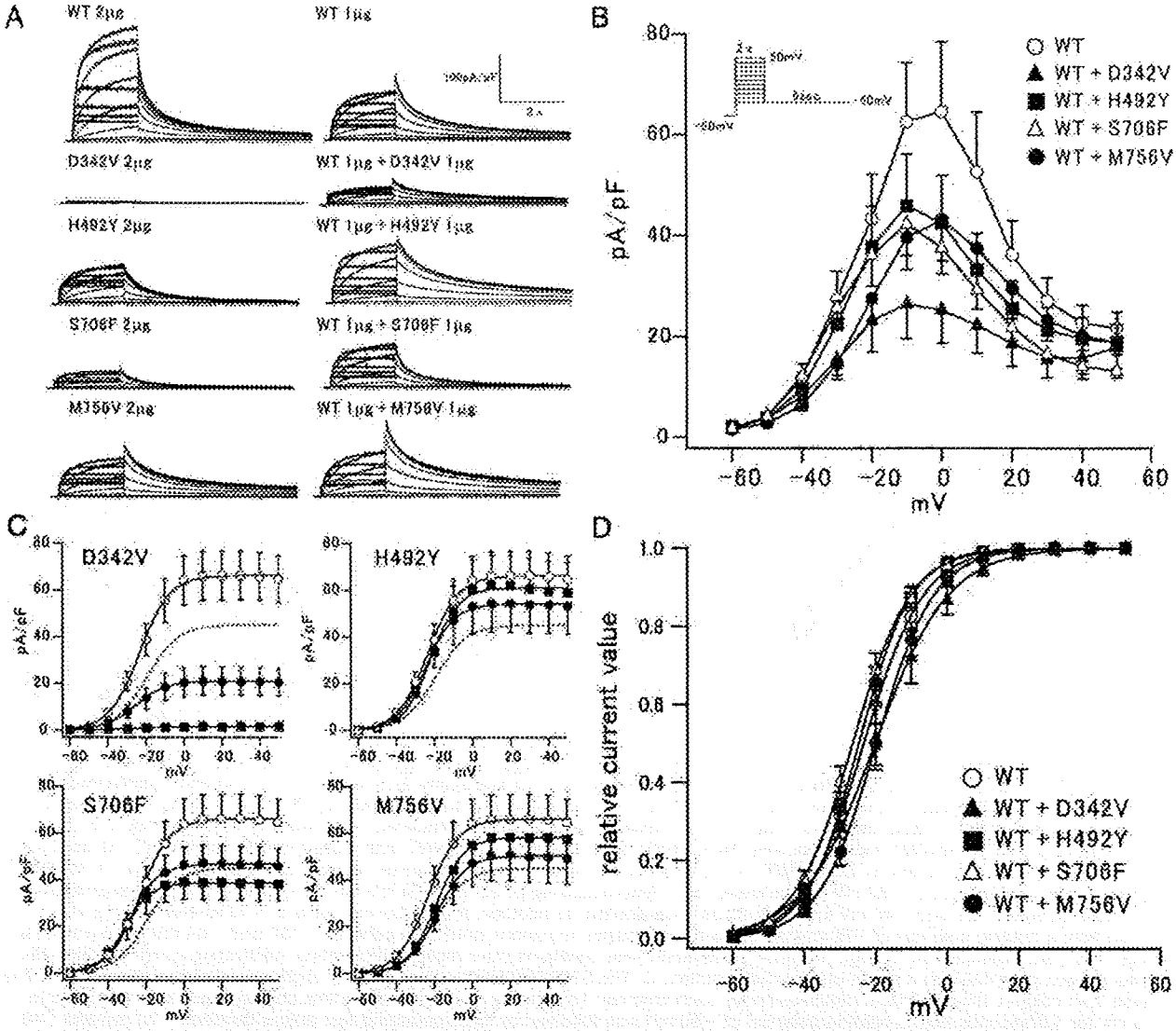

Figure 3. *KCNH2* mutations identified in drug-induced LQT subjects produced various levels of functional effects. A, Current traces of I_{Kr} reconstituted in CHO cells. Expression of the respective clones, indicated above each graph, all displayed I_{Kr}-like currents, except for D342V. Current amplitude was normalized by respective cell capacitance and was indicated as the current density. B, Current-voltage (I-V) relationships for amplitudes of steady-state currents at the end of 2-second depolarizing pulses. Currents were elicited by depolarizing pulses from a holding potential of −80 mV to test potential between −60 to +50 mV (with a 10-mV step increment), followed by repolarization to −60 mV to monitor tail current amplitude. The voltage-clamp protocol is shown in the inset. C, I-V relationships for amplitudes of peak tail currents measured at −60 mV. Open circles, WT (2 μg); filled squares, mutant (2 μg); filled circles, WT (1 μg) plus mutant (1 μg); and dotted lines, WT (1 μg). All data were recorded from 10 to 25 cells. D, Voltage dependence of activation for each channel. The data were fitted to a Boltzmann function.

current densities of D342V/WT (1.5±0.9 pA/pF, $P<0.001$ versus WT) and S706F/WT (38.9±7.3 pA/pF, $P<0.05$ versus WT) channels were significantly smaller than WT. D342V/WT channel displayed currents smaller than WT 1 μg (indicated by dotted line), whereas S706F/WT currents were similar to WT 1 μg in size. Thus, D342V channels had weakly dominant negative suppression effects on reconstituted I_{Kr}-like currents, whereas S706F had no dominant negative suppression effect. To examine the voltage dependence for activation, Boltzmann function curves were fitted to the relationship between peak tail currents and test voltages under respective conditions and are represented by solid lines in Figure 3C. Half inactivation voltages ($V_{1/2}$) were −23.2±1.6 mV for WT, −19.8±3.0 mV for D342V/WT, −24.6±1.4 mV for H492Y/WT, −26.1±1.5 mV for S706F/WT, and −19.8±1.7 mV for M756V/WT, respectively (Figure 3D). Therefore, the mutations did not affect the voltage-dependent activation of the reconstituted I_{Kr}-like channel.

Whether the mutations affected the inactivation kinetics of *KCNH2* channels was then assessed. Figure 4A shows the voltage dependence of availability of WT and mutant channels measured by a brief repolarization method (inset). With a 1-second depolarizing pulse, peak tail current amplitudes (arrow in the inset) after short preconditioning voltage pulses (5 ms) are plotted against the voltage of conditioning pulse. Mutant channels caused significant voltage shift of channel

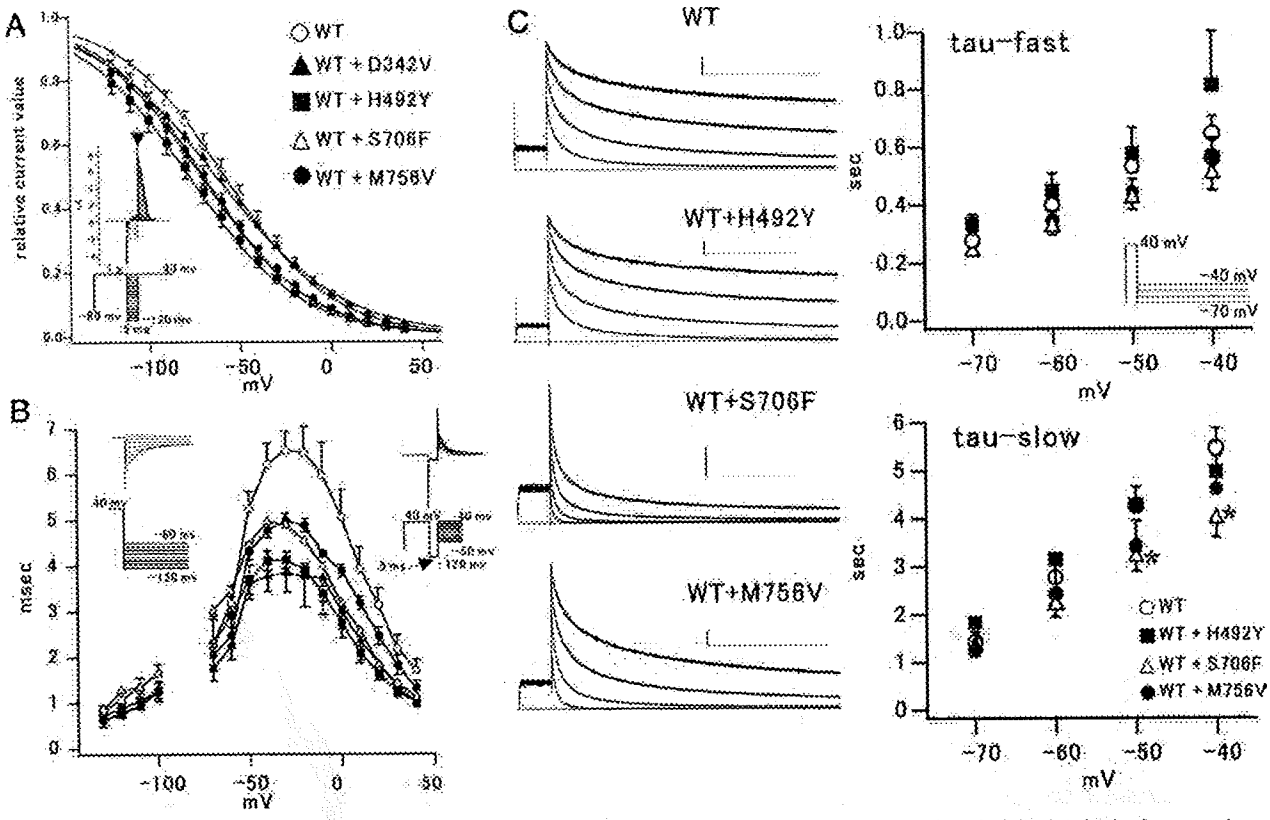

Figure 4. Multiple gating defects associated with KCNH2 mutations. A, Mutations associated with drug-induced arrhythmia caused a negative shift of inactivation gate of *KCNH2* channels. Steady-state channel availability as a function of membrane potential was measured by using a double-step method, as shown in the insets: the voltage-clamp protocol and original current traces from a representative cell expressing WT *KCNH2* channels. Open circles indicate the inactivation calculated from cells expressing cDNA with WT (2 μg), closed triangles, D342V/WT; closed squares, H492Y/WT; open triangles, S706F/WT; and closed circles, M756V/WT. All data were taken from 14 to 20 cells except for D342V/WT. B, To examine the inactivation time course, a conditioning pulse to +40 mV for 900 ms from a holding potential of −80 mV was followed by a hyperpolarizing pulse to −120 mV for 5 ms, and subsequent depolarizing test pulses between −50 and +40 mV in 10 mV steps were applied. In addition, a conditioning pulse to +40 mV for 750 ms was applied from a holding potential of −80 mV, followed by test pulses to various potentials between −130 and −60 mV in 10 mV increments. The inset illustrates the voltage protocol. Inactivation time constants were measured by fitting inactivating currents during test pulses at each potential with a single exponential function. C, The S706F/*KCNH2* mutant channel slightly accelerates deactivation time course. Left column, time course of deactivation for each channel. To examine the deactivation time course, a conditioning pulse to +40 mV for 1.6 seconds from a holding potential of −80 mV was followed by hyperpolarizing test pulses between −70 mV and −40 mV in 10-mV increments for 16 seconds (inset). Currents were not leak-subtracted. Each inset illustrates scale bars of 200-pA and 5-second times. Deactivation time constants (tau) were measured by fitting deactivating currents during test pulses at each potential with double exponentials. The slow components of tau for the S706F/WT channel were smaller than that of WT; **P*<0.05.

availability to the hyperpolarizing direction compared with WT ($V_{1/2}$ of −58.3±4.7 mV for WT, $V_{1/2}$ of −61.4±6.5 mV for D342V/WT, −77.8±4.7 mV for H492Y/WT, −70.1±3.2 mV for S706F/WT, and −71.1±4.6 mV for M756V/WT, respectively). The time course to recovery from or the development of the inactivation (recovery from inactivation at hyperpolarized potentials and development of inactivation at >−70 mV) was analyzed by double or triple pulse protocols. The time course of inactivating kinetics could be fitted by a single-exponential function. Time constants thus calculated were significantly smaller than WT and mutant channels over a wide range of voltage (between −50 and +40 mV for D342V/WT and H492Y/WT; between −30 and +20 mV for S706F/WT; between −40 and 0 mV for M756V/WT, Figure 4B). These results demonstrate that drug-induced LQTS mutants have accelerated inactivation kinetics. Figure 4C shows representative families of current traces (left panel) and time constants (right panel) of deactivation in each channel. When the time course of deactivating kinetics was fitted by a double-exponential function, the S706F/WT channel slightly accelerated the deactivation process (Figure 4C).

Most of the drugs that induced LQTS in the study subjects have been known to block I_{Kr} in a concentration-dependent manner,[8,17,19–22] whereas I_{Kr} channel with *KCNH2* mutations may have different drug sensitivities compared with the WT channel. Figure 5 shows 3 sets of drug concentration-current inhibition relationships associated with *KCNH2* mutations with respect to erythromycin (5A), disopyramide (5B), and pirmenol (5C). In each case of drug-induced LQTS, an electrophysiological assay of current inhibition by the respective culprit drug was performed, for example, hydroxyzine,[17] erythromycin, disopyramide, and pirmenol. IC_{50}s were not significantly different between WT and the respective mutant channels, suggesting that a change in drug sensitivity was not involved in causing the drug-induced TdP in the study subjects.

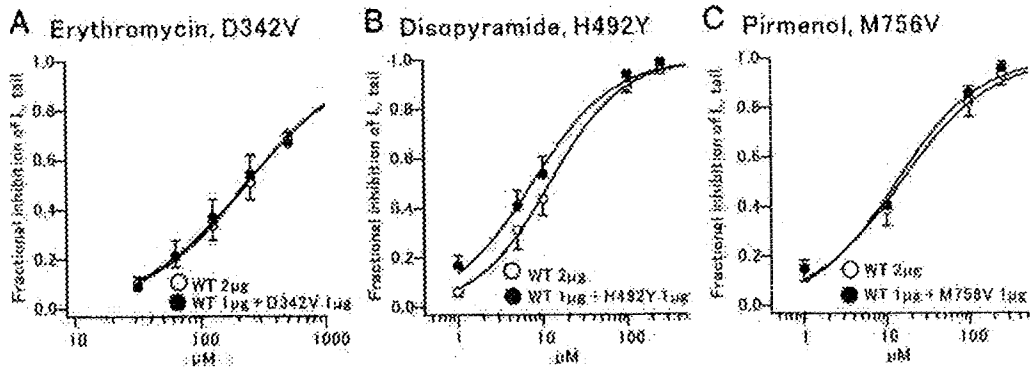

Figure 5. Both WT and mutant channels showed similar drug sensitivities to the culprit agents. A, Fractional blockade by micromolar erythromycin was recorded with regard to D342V/WT or WT as described in the methods and is plotted against the drug concentrations. B, Similarly, the relationship between the fractional block by disopyramide and its concentration are shown. C, The relationship between the fractional pirmenol block of M756V/WT or WT channels and its concentration. IC_{50}s for erythromycin, disopyramide, and pirmenol were 327 μmol/L (WT) and 248 μmol/L (D342V/WT), 13.9 μmol/L (WT) and 8.4 μmol/L (H492Y/WT), and 16.6 μmol/L (WT) and 13.4 μmol/L (M756V/WT), respectively (n=4 or 5 cells per condition).

Computer Simulation of Ventricular Action Potentials

To compare how the functional changes caused by mutants affect ventricular action potentials, a simulation study was conducted using the Luo-Rudy computer model that incorporated the Markov[16] or Hodgkin-Huxley[23] process gating for the mutant channels (Figure 6A). Table 2 shows parameters of simulation that have been changed to fit to experimental results. First, the I_{Kr} or I_{Ks} conductance was reduced to the level observed in the D342V/WT, A614V/WT, and R231C/WT channels. The deactivation time course for R231C/WT was also fitted by modifying a parameter. Second, the transition rate was changed accordingly from inactivation to open states (αi) and fitted with the experimental data seen in H492Y/WT and M756V/WT channels. Acceleration of inactivation induced by modifying the transition rate αi reproduced smaller amplitudes for I-V relationships and negative shift of steady-state inactivation curve (Figure 4A); these findings were compatible with the experimental results (Figure 3, A through C). Third, some parameters were altered to simulate the S706F/WT model, by reducing the I_{Kr} conductance, modifying αi, and increasing the transition rate from open to deactivation states. This was followed by change to parameters associated with the activation and deactivation rates for the R243H/WT model. Finally, not only was I_{Na} conductance decreased in the subjects, but the burst mode was also added to simulate the sustained current for the L1825P model.[24] The L1825P/WT channel was heterogeneously simulated to equally mix WT and L1825P models.

In the simulated M cells using the Luo-Rudy model, the order of increase in magnitude of action potential duration (APD) was A614V/WT>R231C/WT>D342V/WT>S706S/WT>R243H/WT=L1825P/WT >H492Y/WT>M756V/WT for dLQTS mutations (Figure 6B, middle panel). Typically, for cLQTS mutations, the simulated APD was longer than for WT or drug-induced models, whereas APDs in drug-induced models were intermediate between those in WT and those in cLQTS (clinical information for simulated cLQTS are presented in supplemental Table 1).

Finally, an effort was made to reproduce action potentials in the presence of I_{Kr}-blocking drugs (Figure 6C). Early afterdepolarizations appeared in all mutants where there were smaller reductions in the I_{Kr} conductance compared with the corresponding WT. Because drug sensitivities for WT and mutant channels were not different (Figure 5), the same inhibition rate was used in both the WT and mutant models and the I_{Kr} conductance was gradually reduced at the cycle length of 1200 ms. As shown in Figure 6C, typically, when the I_{Kr} conductance was theoretically decreased to 89% of the basal conductance for each channel, the D342V/WT model began to develop early afterdepolarizations, whereas the WT model produced only a 2.9% increase in APD.

Discussion

There were 3 major findings.[1] In 8 of 20 consecutive dLQTS subjects, 5 *KCNH2,* 2 *KCNQ1,* and 1 *SCN5A* heterozygous missense mutations were identified; there was a similar positive mutation rate with dLQTS compared with cLQTS.[2] Both *KCNQ1* and *KCNH2* mutants possessed loss of function effects on reconstituted I_{Ks}- or I_{Kr}-like channels.[3] The functional changes in mutant channels reconstituted by the computer simulation resulted in a mildly prolonged APD, suggesting that the dLQTS may partially have a genetic background, especially mild or latent long-QT syndrome–associated mutations.

Mutations in dLQTS

Potential torsadegenic drugs are used in the clinical setting and include antiarrhythmic drugs, antibiotics, antihistamines, psychiatric drugs, and cholinergic antagonists. These might induce TdP, which may lead to the sudden cardiac death of individuals whose QT intervals were within normal range before taking the drug. Several drugs such as cisapride and terfenadine have been withdrawn from the market because of these possible side effects.[25,26] The incidence of dLQTS is not high, and the drugs lead to TdP in only a small percentage of individuals, suggesting that there may be an underlying genetic background that predisposes these individuals to the risk.

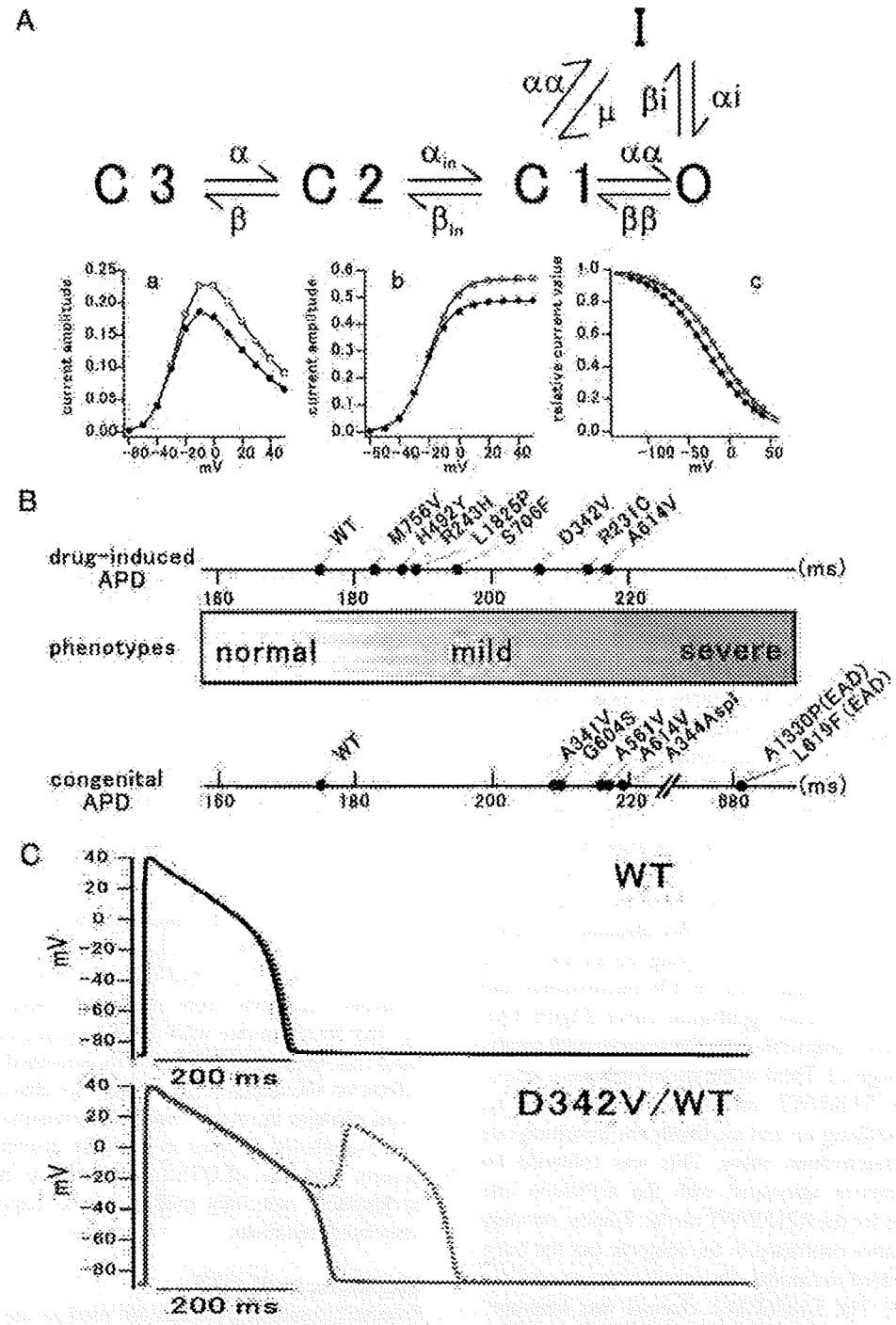

Figure 6. Simulation study of congenital and dLQTS-associated channels. A, Scheme showing a Markov model for I_{Kr} channels and simulation results for voltage-clamp protocols with a modified the transition rate αi; $\alpha i = 0.439 \times \exp(-0.02352 \times (V + 40))/K_{out}$. The 3 panels illustrate the result on the M756V/WT model, (a); the I-V relationship, (b); the I-V relationship for amplitudes of peak tail currents and (c); the steady-state inactivation curves. Open circles, WT; filled circles, mutant. B, Simulation study of action potential durations (APD). The parameters used for simulation were changed and matched the experimental results for voltage-clamp protocols. Myocardium models were stimulated at the cycle length of 600 ms for 5 minutes. C, Simulated APDs with I_{Kr}-blocking effects. When I_{Kr} conductance was decreased to 11% in each of the models, the D342V model showed early afterdepolarization, whereas the WT model had only slight prolonged APD. Bold lines, controls; dotted lines, models with I_{Kr}-blocking effects.

In the medical literature, 13 *KCNQ1* or *KCNH2* mutations (13 of 15 mutations, 87%) associated with dLQTS, including 6 of the mutations identified in this present study, have been located in nonpore regions (Figure 1B). Mutations in nontransmembrane regions have been shown to cause either mild long-QT syndrome or benign clinical phenotypes.[27] Mutation sites may influence the clinical and basic electrophysiological characteristics of patients with dLQTS. It is of interest that

Table 2. Parameters of Simulation Data in LQTS

Phenotype	Gene	Mutant	WT Basal Parameters	Mutant Changed Parameters
dLQTS	*KCNQ1*	R231C	gks=0.202*(1+0.6/(1+pow((0.000038/cai), 1.4)))	gks=0.103*(1+0.6/(1+pow((0.000038/cai), 1.4)))
			tauxs1=1/(0.0000719*(v+30)/(1−exp(−0.148...	tauxs1=1.1/(0.0000719*(v+30)/(1−exp(−0.148...
dLQTS	*KCNQ1*	R243H	xs1ss=1/(1+exp(− (v−1.5)/16.7))	xs1ss=1/(1+exp(− (v−11.5)/16.7))
			tauxs1=1/(0.0000719*(v+30)/(1−exp(−0.148...	tauxs1=0.9/(0.0000719*(v+30)/(1−exp(−0.148...
dLQTS	*KCNH2*	D342V	gherg=0.0135*pow(Kout, 0.59)	gherg=0.0043*pow(Kout, 0.59)
dLQTS	*KCNH2*	H492Y	αi=0.439*exp(−0.02352*(v+25))*4.5/Kout	αi=0.439*exp(−0.02352*(v+47))*4.5/Kout
dLQTS	*KCNH2*	S706F	gherg=0.0135*pow(Kout, 0.59)	gherg=0.0096*pow(Kout, 0.59)
			αi=0.439*exp(−0.02352*(v+25))*4.5/Kout	αi=0.439*exp(−0.02352*(v+39))*4.5/Kout
			bβ=2.9375e-3*exp(−0.02158*v)	bβ=5.875e-3*exp(−0.02158*v)
dLQTS	*KCNH2*	M756V	αi=0.439*exp(−0.02352*(v+25))*4.5/Kout	αi=0.439*exp(−0.02352*(v+40))*4.5/Kout
dLQTS	*KCNH2*	A614V	gherg=0.0135*pow(Kout, 0.59)	gherg=0.0024*pow(Kout, 0.59)
dLQTS	*SCN5A*	L1825P	G_{Na}=16	G_{Na}=1.76
			No burst mode	α6=5*e-6
			No burst mode	β6=3.34*e-4
cLQTS	*KCNQ1*	A341V	gks=0.202*(1+0.6/(1+pow((0.000038/cai), 1.4)))	gks=0.101*(1+0.6/(1+pow((0.000038/cai), 1.4)))
cLQTS	*KCNQ1*	A344AspI	gks=0.202*(1+0.6/(1+pow((0.000038/cai), 1.4)))	gks=0.087*(1+0.6/(1+pow((0.000038/cai), 1.4)))
cLQTS	*KCNH2*	A561V	gherg=0.0135*pow(Kout, 0.59)	gherg=0.0023*pow(Kout, 0.59)
			aα=65.5e-3*exp(0.05547153*(v−36))	aα=65.5e-3*exp(0.05547153*(v-16))
cLQTS	*KCNH2*	G604S	gherg=0.0135*pow(Kout, 0.59)	gherg=0.0040*pow(Kout, 0.59)
			αi=0.439*exp(−0.02352*(v+25))*4.5/Kout	αi=0.439*exp(−0.02352*(v+35))*4.5/Kout
cLQTS	*KCNH2*	A614V	gherg=0.0135*pow(Kout, 0.59)	gherg=0.0024*pow(Kout, 0.59)
cLQTS	*SCN5A*	L619F	G_{Na}=16	G_{Na}=6.24
			No burst mode	α6=10*e-6
			No burst mode	β6=3*e-4
cLQTS	*SCN5A*	L1330P	G_{Na}=16	G_{Na}=6.24
			No burst mode	α6=10*e-6
			No burst mode	β6=3*e-4

the functional assay of our 7 mutations resulted in various levels of loss of function, but most of them showed no dominant negative suppression, which is usually observed in the classic cLQTS. Clinical characteristics during the drug intake were not significantly distinct from those of cLQTS, which shares a similar genetic background with the dLQTS. Several polymorphisms have been shown to be associated with dLQTS.[4,28] Abbott et al[4] identified a polymorphism (T8A) of the *KCNE2* gene encoding MiRP, a β-subunit for the I_{Kr} channel, which is present in 1.6% of the population and is associated with TdP induced by quinidine or sulfamethoxazole/trimethoprim administration. Splawski et al[28] also found a heterozygous polymorphism involving substitution of serine with tyrosine (S1102Y) in the sodium channel gene *SCN5A* among blacks that increased the risk for drug-induced TdP. The polymorphism was present in 57% of 23 patients with proarrhythmic episodes but in only 13% of control subjects. These findings suggested that common genetic variations may increase the risk for development of drug-related arrhythmias.

Roden et al[29] reported that cisapride could rescue trafficking of L1825P channel with a potentially sustained current and revealed a new mechanism of dLQTS with the Luo-Rudy model. However, in the genotyped subjects in the present study, dLQTS mainly resulted from the I_{Kr}-blocking effect of culprit drugs in the presence of latent genetic backgrounds. Cardiac repolarization reserve may protect subjects against the drug-induced QT prolongation by I_{Kr}-blocking drugs.[30,31] In the presence of latent genetic backgrounds, however, reduction in the repolarization reserve unveils the presence of so-called "concealed" long-QT syndrome when drugs with I_{Kr}-blocking effects are administered. The presence of borderline prolongation of the QT interval, together with personal information such as unexplained previous syncope and family history of premature sudden death, may help to prevent drug-induced arrhythmia even if a subject's Schwartz score is low, because they could have a potential risk of TdP. Special attention should be paid to family members of the index subject with drug-induced QT prolongation because ≈30% of family members were found to have a predisposing genetic background in the present study. Indeed, they may have inherited the risk for being susceptible to dLQTS.

Limitations of the Study

This study has some limitations. Bacause of the small cohort of dLQTS subjects, this study was not powered to quantify the overall prevalence of ion channel mutations in the group of subjects with drug-induced TdP; there was also a possible

selection bias in the population. As for the causative agents, we were unable to test the action of amphetamine and methamphetamine because it was impossible to obtain these illegal drugs for clinical study. However, a previous report has shown that 3,4-methylenedioxy methamphetamine (ecstasy, NMDA) prolongs the APD of hippocampal neurons by blocking the conductance of a resting K^+ channel.[32] It is quite possible that these drugs also suppressed cardiac K^+ currents and induced QT prolongation and TdP in 1 subject in our study, based on her medical records. Regarding protein trafficking, 2 mutations in this study, A614V in *KCNH2*[17] and L1825P in *SCN5A*,[29] had been reported to be trafficking-deficient mutations. Though protein trafficking of other mutants remains unclear, especially R243H in *KCNQ1*, and H492Y, S706F, and M756V in *KCNH2*, would be not trafficking-deficient because, under heterozygous conditions, these mutants showed adequate current density compared with WT. In the simulation study, the parameter settings could mimic mutant channels. In addition, the setting of the parameters might have innumerable patterns, and it therefore remains possible that other combinations of patterns could also simulate mutant channels.

Acknowledgments

We thank Arisa Ikeda for excellent technical assistance.

Sources of Funding

This work was supported by the Grant-in-Aid for Scientific Research from the Japan Society for the Promotion of Science and the Biosimulation and Health Sciences Research Grant (H18-Research on human Genome-002) from the Ministry of Health, Labor, and Welfare of Japan (M.H.) and a Grant-in-Aid for Young Scientists from the Ministry of Education, Culture and Technology of Japan (H.I.).

Disclosures

None

References

1. Schwartz PJ, Periti M, Malliani A. The long QT syndrome. *Am Heart J.* 1975;89:378–390.
2. Moss AJ, Schwartz PJ, Crampton RS, Tzivoni D, Locati EH, MacCluer J, Hall WJ, Weitkamp L, Vincent GM, Garson A Jr. The long-QT syndrome: prospective longitudinal study of 328 families. *Circulation.* 1991;84:1136–1144.
3. Haverkamp W, Breithardt G, Camm AJ, Janse MJ, Rosen MR, Antzelevitch C, Escande D, Franz M, Malik M, Moss A, Shah R. The potential for QT prolongation and proarrhythmia by non-antiarrhythmic drugs: clinical and regulatory implications: report on a policy conference of the European Society of Cardiology. *Eur Heart J.* 2000;21:1216–1231.
4. Sesti F, Abbott GW, Wei J, Murray KT, Saksena S, Schwartz PJ, Priori SG, Roden DM, George AL Jr, Goldstein SA. A common polymorphism associated with antibiotic-induced cardiac arrhythmia. *Proc Natl Acad Sci U S A.* 2000;97:10613–10618.
5. Makita N, Horie M, Nakamura T, Ai T, Sasaki K, Yokoi H, Sakurai M, Sakuma I, Otani H, Sawa H, Kitabatake A. Drug-induced long-QT syndrome associated with a subclinical SCN5A mutation. *Circulation.* 2002;106:1269–1274.
6. Napolitano C, Schwartz PJ, Brown AM, Ronchetti E, Bianchi L, Pinnavaia A, Acquaro G, Priori SG. Evidence of a cardiac ion channel mutation underlying drug-induced QT prolongation and life-threatening arrhythmias. *J Cadiovasc Electrophysiol.* 2000;11:691–696.
7. Yang P, Kanki H, Drolet B, Yang T, Wei J, Viswanathan PC, Hohnloser SH, Shimizu W, Schwartz PJ, Stanton M, Murray KT, Norris K, George AL, Roden DM. Allelic variants in long-QT disease genes in patients with drug-associated torsades de pointes. *Circulation.* 2002;105:1943–1948.
8. Hayashi K, Shimizu M, Ino H, Yamaguchi M, Terai H, Hoshi H, Higashida H, Terashima N, Uno Y, Kanaya H, Mabuchi H. Probucol aggravates long QT syndrome associated with a novel missense mutation M124T in the N-terminus of HERG. *Clin Sci (Lond).* 2004;107:175–182.
9. Bellocq C, Wilders R, Schott JJ, Louérat-Oriou B, Boisseau P, Le Marec H, Escande D, Baró I. A common antitussive drug, clobutinol, precipitates the long QT syndrome. *Mol Pharmacol.* 2004;66:1093–1102.
10. Lehtonen A, Fodstad H, Laitinen-Forsblom P, Toivonen L, Kontula K, Swan H. Further evidence of inherited long QT syndrome gene mutations in antiarrhythmic drug-induced torsades de pointes. *Heart Rhythm.* 2007;4:603–607.
11. Haverkamp W, Shenasa M, Borggrefe M, Breithardt G. *Cardiac Electrophysiology.* 4th ed. Philadelphia: Saunders; 1999:886–899.
12. Bazett HC. An analysis of the time relations of electrocardiograms. *Heart.* 1920;7:353–370.
13. Schwartz PJ, Moss AJ, Vincent GM, Crampton RS. Diagnostic criteria for the long QT syndrome: an update. *Circulation.* 1993;88:782–784.
14. Ohno S, Zankov DP, Yoshida H, Tsuji K, Makiyama T, Itoh H, Akao M, Hancox JC, Kita T, Horie M. N- and C-terminal KCNE1 mutations cause distinct phenotypes of long QT syndrome. *Heart Rhythm.* 2007;4:332–340.
15. Splawski I, Shen J, Timothy KW, Vincent GM, Lehmann MH, Keating MT. Genomic structure of three long QT syndrome genes: KVLQT1, HERG, and KCNE1. *Genomics.* 1998;51:86–97.
16. Clancy CE, Rudy Y. Cellular consequences of HERG mutations in the long QT syndrome: precursors to sudden cardiac death. *Cardiovasc Res.* 2001;50:301–313.
17. Sakaguchi T, Itoh H, Ding WG, Tsuji K, Nagaoka I, Oka Y, Ashihara T, Ito M, Yumoto Y, Kubota T, Zenda N, Higashi Y, Takeyama Y, Matsuura H, Horie M. Hydroxyzine, an H_1 receptor antagonist of first generation, inhibits reconstituted I_{Kr} currents. *J Pharmacol Sci.* 2008;108:462–471.
18. Nakajima T, Furukawa T, Tanaka T, Katayama Y, Nagai R, Nakamurea Y, Hiraoka M. Novel mechanism of HERG current suppression in LQT2: shift in voltage dependence of HERG inactivation. *Circ Res.* 1998;83:415–422.
19. Daleau P, Lessard E, Groleau MF, Turgeon J. Erythromycin blocks the rapid component of the delayed rectifier potassium current and lengthens repolarization of guinea pig ventricular myocytes. *Circulation.* 1995;91:3010–3016.
20. Paul AA, Witchel HJ, Hancox JC. Inhibition of HERG potassium channel current by the class Ia antiarrhythmic agent disopyramide. *Biochem Biophys Res Commun.* 2001;280:1243–1250.
21. Yoshida H, Horie M, Otani H, Takano H, Tsuji K, Kubota T, Fukunami M, Sasayama S. Characterization of a novel missense mutation in the pore of HERG in a patient with long QT syndrome. *J Cardiovasc Electrophysiol.* 1999;10:1262–1270.
22. Walker BD, Singleton CB, Bursill JA, Wyse KR, Valenzuela SM, Qiu MR, Breit SN, Campbell TJ. Inhibition of the human ether-a-go-go-related gene (HERG) potassium channel by cisapride: affinity for open and inactivated states. *Br J Pharmacol.* 1999;128:444–450.
23. Hodgkin AL, Huxley AF. A quantitative description of membrane current and its application to conduction and excitation in nerve. *J Physiol.* 1952;117:500–544.
24. Clancy CE, Rudy Y. Na+ channel mutation that causes both Brugada and long-QT syndrome phenotypes: a simulation study of mechanism. *Circulation.* 2002;105:1208–1213.
25. Wysowski DK, Bacsanyi J. Cisapride and fatal arrhythmia. *N Engl J Med.* 1996;335:290–291.
26. Monahan BP, Ferguson CL, Killeavy ES, Lloyd BK, Troy J, Cantilena LR Jr. Torsades de pointes occurring in association with terfenadine use. *JAMA.* 1990;264:2788–2790.
27. Donger C, Denjoy I, Berthet M, Neyroud N, Cruaud C, Bennaceur M, Chivoret G, Schwartz K, Coumel P, Guicheney P. KVLQT1 C-terminal missense mutation causes a forme fruste long-QT syndrome. *Circulation.* 1997;96:2778–2781.
28. Splawski I, Timothy KW, Tateyama M, Clancy CE, Malhotra A, Beggs AH, Cappuccio FP, Sagnella GA, Kass RS, Keating MT. Variants of

SCN5A sodium channel implicated in risk of cardiac arrhythmia. *Science*. 2002;297:1333–1336.
29. Liu K, Yang T, Viswanathan PC, Roden DM. New mechanism contributing to drug-induced arrhythmia: rescue of a misprocessed LQT3 mutant. *Circulation*. 2005;112:3239–3246.
30. Jost N, Virág L, Bitay M, Takács J, Lengyel C, Biliczki P, Nagy Z, Bogáts G, Lathrop DA, Papp JG, Varró A. Restricting excessive cardiac action potential and QT prolongation: a vital role for IKs in human ventricular muscle. *Circulation*. 2005;112:1392–1399.
31. Roden DM, Yang T. Protecting the heart against arrhythmias: potassium current physiology and repolarization reserve. *Circulation*. 2005;112:1376–1378.
32. Premkumar L, Ahern G. Blockade of a resting potassium channel and modulation of synaptic transmission by ecstasy in the hippocampus. *J Pharmacol Exp Ther*. 1995;274:718–722.

CLINICAL PERSPECTIVE

Drug-induced long-QT syndrome (dLQTS) is a disease associated with the appearance of a prolonged QT interval and torsades de pointes after taking a culprit drug or drugs; the QT interval usually returns to within normal range after a washout period of these drugs. The clinical phenotype of dLQTS that appears during administration of these drugs resembles that of congenital long-QT syndrome (cLQTS), and "latent" genetic factors may underlie the susceptibility of a subject to drug-induced serious adverse reactions, such as a long QT interval and torsades de pointes. In the analysis of cLQTS-associated genes encoding cardiac ion channel-composing proteins, this study revealed that dLQTS had a similar positive mutation rate compared with cLQTS. When reconstituted in Chinese hamster ovary cells, *KCNQ1* and *KCNH2* mutant channels showed complex gating defects without dominant negative effects or a relatively mild decreased current density. With the Luo-Rudy simulation model of action potentials, action potential durations of most mutant channels were between those of wild-type and cLQTS. In conclusion, although the dLQTS subjects had genetic backgrounds that were similar to cLQTS subjects, the functional changes associated with these mutations identified in dLQTS were different from those in cLQTS. Thus, we believe that dLQTS can be regarded as a latent form of long-QT syndrome. When I_{Kr}-blocking agents produce excessive QT prolongation, the underlying genetic background of the dLQTS subject should be taken into consideration, as would be the case with cLQTS.

RESEARCH ARTICLE

Human Mutation

OFFICIAL JOURNAL
HGVS
HUMAN GENOME VARIATION SOCIETY
www.hgvs.org

Novel KCNE3 Mutation Reduces Repolarizing Potassium Current and Associated With Long QT Syndrome

Seiko Ohno,[1] Futoshi Toyoda,[2] Dimitar P Zankov,[2,3] Hidetada Yoshida,[1] Takeru Makiyama,[1] Keiko Tsuji,[3] Toshihiro Honda,[4] Kazuhiko Obayashi,[5] Hisao Ueyama,[6] Wataru Shimizu,[7] Yoshihiro Miyamoto,[8] Shiro Kamakura,[7] Hiroshi Matsuura,[2] Toru Kita,[1] and Minoru Horie[3]*

[1]*Department of Cardiovascular Medicine, Kyoto University Graduate School of Medicine, Kyoto, Japan*

[2]*Department of Physiology, Shiga University of Medical Science, Shiga, Japan*

[3]*Department of Cardiovascular and Respiratory Medicine, Shiga University of Medical Science, Shiga, Japan*

[4]*Cardiovascular Center, Saiseikai Kumamoto Hospital, Kumamoto, Japan*

[5]*Obayashi Clinic, Kyoto, Japan*

[6]*Department of Molecular Medical Biochemistry, Shiga University of Medical Science, Shiga, Japan*

[7]*Division of Cardiology, Department of Internal Medicine, National Cardiovascular Center, Osaka, Japan*

[8]*Laboratory of Molecular Genetics, National Cardiovascular Center, Osaka, Japan*

Communicated by Claude Férec

Received 25 January 2008; accepted revised manuscript 5 May 2008.
Published online 20 March 2009 in Wiley InterScience (www.interscience.wiley.com). DOI 10.1002/humu.20834

ABSTRACT: Long QT syndrome (LQTS) is an inherited disease involving mutations in the genes encoding a number of cardiac ion channels and a membrane adaptor protein. Among the genes that are responsible for LQTS, *KCNE1* and *KCNE2* are members of the *KCNE* family of genes, and function as ancillary subunits of Kv channels. The third *KCNE* gene, *KCNE3*, is expressed in cardiac myocytes and interacts with *KCNQ1* to change the channel properties. However, *KCNE3* has never been linked to LQTS. To investigate the association between *KCNE3* and LQTS, we conducted a genetic screening of *KCNE3* mutations and single nucleotide polymorphisms (SNPs) in 485 Japanese LQTS probands using DHPLC-WAVE system and direct sequencing. Consequently, we identified two *KCNE3* missense mutations, located in the N- and C-terminal domains. The functional effects of these mutations were examined by heterologous expression systems using CHO cells stably expressing KCNQ1. One mutation, p.R99λH was identified in a 76-year-old woman who suffered torsades de pointes (TdP) after administration of disopyramide. Another mutation, p.T4A was identified in a 16-year-old boy and 67-year-old woman. Although the boy carried another *KCNH2* mutation, he was asymptomatic. On the other hand, the woman suffered from hypokalemia-induced TdP. In a series of electrophysiological analyses, the KCNQ1(Q1) +KCNE3(E3)-R99λH channel significantly reduced outward current compared to Q1+E3-WT, though the current density of the Q1+E3-T4A channel displayed no statistical significance. This is the first report of *KCNE3* mutations associated with LQTS. Screening for variants in the *KCNE3* gene is of clinical importance for LQTS patients.
Hum Mutat 30, 557–563, 2009. © 2009 Wiley-Liss, Inc.

KEY WORDS: long QT syndrome; LQTS; *KCNE3*; ion channel; molecular screening; electrophysiology

Introduction

Long QT syndrome (LQTS) is an inherited disease characterized by a prolonged QT interval and a high risk of sudden cardiac death due to peculiar ventricular tachycardia known as torsades de pointes (TdP) [Moss and Kass, 2005]. Most of the LQTS-causing genes encode ion channels, with particular regard to potassium (K) channels. Among them, *KCNE1* (E1) and *KCNE2* (E2) are members of the *KCNE* family (E1 through *KCNE5*) encoding a single-transmembrane-domain proteins. They are called MinK-related peptides (MiRPs) that function as ancillary subunits of Kv channels. In 1999, the third *KCNE* gene, *KCNE3* (ONIM *604433) (E3), was cloned by homology to E1 [Abbott et al., 1999]. In the functional analysis on the KCNQ1 (Q1) +E3 channel, E3 was shown to markedly change Q1 channel properties to yield those activating nearly instantaneously and linearly on voltage [Schroeder et al., 2000].

The expression of E3 in heart was examined and confirmed by northern blot analysis [Schroeder et al., 2000], real-time quantitative RT-PCR [Bendahhou et al., 2005; Lundquist et al., 2005, 2006] and in situ hybridization [Lundquist et al., 2005]. E3 was expressed in all regions of the human heart including left and right ventricles [Lundquist et al., 2005]. The expression level of E3 was larger than that of E2 in every region of the human heart, although smaller than that of E1 [Bendahhou et al., 2005; Lundquist et al., 2005, 2006]. Recently, E3 was reported to

S.O. and F.T. contributed equally to this work.

*Correspondence to: Minoru Horie, M.D., Ph.D., Department of Cardiovascular and Respiratory Medicine, Shiga University of Medical Science, Seta Tsukinowa-cho, Otsu, Shiga, Japan 520-2192. E-mail: horie@belle.shiga-med.ac.jp

Contract grant sponsor: Japan Society for the Promotion of Science; Contract grant sponsor: Ministry of Health, Labour and Welfare, Japan; Grant number: H18-Research on Human Genome-002.

establish a complex with Q1 along with E1 [Morin and Kobertz, 2007]. The Q1+E1+E3 complex generated the current with the combined properties of homomeric Q1+E1 and Q1+E3 complexes, as we previously reported the properties of Q1+E1+E2 complexes [Toyoda et al., 2006]. Taken together, the dysfunction of the Q1+E3 channel may reduce repolarizing K currents in the myocardium, which thereby prolongs the QT interval, although Q1–E3 channels have not yet been demonstrated in the heart.

Abbott et al. [2001] demonstrated a missense mutation of E3 (p.R83λH) in the patients of periodic paralysis. The reduced current densities of the E3-R83λH plus Kv3.4 complex channel in the skeletal muscle caused periodic paralysis, though the authors did not mention cardiac symptoms. More recently, Lundby et al. [2008] identified an E3 mutation (p.V17λM) from an early-onset lone atrial fibrillation (AF) patients. They performed functional analysis of E3-V17λM in coexpression with five kinds of potassium channels. As a result, they revealed increased activity of KV4.3+E3-V17λM and KCNH2+E3-V17λM channels.

During the genetic screening on 485 Japanese LQTS probands, we identified two novel E3 mutations and one reported single nucleotide polymorphism (SNP) (rs34604640:C>G; p.P39R). The mutations were p.T4A in the N-terminal and p.R99λH in the C-terminal. In the present study, we describe the clinical phenotypes of E3-related LQTS patients and the electrophysiological effects caused by these E3 mutations, and assess the probability of E3 as a candidate gene for LQTS.

Materials and Methods

Subjects

Study patients are comprised of 485 congenital and acquired LQTS probands showing prolongation of the QT interval (QTc≥460 ms) or documented TdP from 485 unrelated families. They were referred consecutively to either of our laboratories for genetic evaluation. All subjects submitted written informed consent in accordance with the guidelines approved by each institutional review board. Each underwent detailed clinical and cardiovascular examinations, and were then characterized on the basis of the QT interval in lead V_5 corrected for heart rate (QTc) according to Bazett's formula and the presence of cardiac symptoms.

Genotyping

Genomic DNA was isolated from venous blood lymphocytes as previously described [Ohno et al., 2007]. Through PCR, denaturing high-performance liquid chromatography (DHPLC), and direct DNA sequencing, we performed a comprehensive open reading frame/splice-site mutational analysis of known LQTS genes (*KCNQ1*, *KCNH2*, *SCN5A*, *KCNE1*, and *KCNE2*) using previously described primers [Ohno et al., 2007]. We did not conduct mutational analysis of *ANKB*, *KCNJ2*, *CACNA1C*, *CAV3*, and *SCN4B*. The *KCNE3* coding region was amplified with a primer pair; forward primer; 5′-CTGAGCTTCTACCGAGTCTT-3′ and reverse primer; 5′-TGCAGTCCACAGCAGAGTTC-3′. The size of the PCR product was 435 base pairs. DHPLC analysis of *KCNE3* was performed at three different temperatures; 59.0, 61.2, and 63.5°C. The cDNA sequence was based on GenBank reference sequence NM_005472.4, and the numbering reflects cDNA numbering with +1 corresponding to the A of the ATG translation initiation codon in the reference sequence, according to journal guidelines. The initiation codon is codon 1.

Plasmid Construction

cDNA for human *KCNE3* (NM_005472.4) was cloned into a PCR3.1 plasmid. Variant amino acid residues were constructed using a Quick Change® II XL Site-Directed Mutagenesis Kit (Stratagene, La Jolla, CA), according to the manufacturer's instructions. Nucleotide sequence analysis was performed on each variant construct prior to the expression study.

Construction of a CHO Cell Line Stably Expressing Human KCNQ1

Flp-In CHO cells containing a single integrated Flp recombinase target (FRT) site at a transcriptionally active locus (Invitrogen, Carlsbad, CA) were used for the generation of a stable KCNQ1 cell line. The full-length cDNA fragment of human *KCNQ1* (GenBank AF000571.1) in a pCI vector (a kind gift from Dr. J. Barhanin, Institut de Pharmacologie Moléculaire et Cellulaire, CNRS, Valbonne, France) was subcloned into a pcDNA5/FRT vector (Invitrogen). This construct was cotransfected into Flp-In CHO cells with pOG44, a Flp-recombinase expression vector (Invitrogen), resulting in the targeting interaction of the expression vector. Stable cell clones were selected in hygromycin B (500 μg/ml; Invitrogen), and the expression of KCNQ1 was tested by the whole-cell patch-clamp recording method. One cell line exhibited uniform and homogenous expression of KCNQ1 currents and was used for experiments.

Cell Culture and Transient Transfection

The stable KCNQ1-CHO cell line was maintained in Ham's F-12 medium supplemented with 10% fetal calf serum and 500 &mug/ml hygromycin B in a humidified incubator gassed with 5% CO_2 and 95% air at 37°C. Before transfection, cells were seeded onto 35-mm plastic culture dishes with seven to eight glass coverslips (5λmm × 3λmm) and incubated for 24 to 48λhr. Transient transfection was performed using Lipofectamine (Invitrogen). The amounts of each cDNA used for transfection were (mug/dish): 1.0 *KCNE3*, and 0.5 green fluorescent protein (GFP). At 48 to 72λhr after transfection, only GFP-positive cells were selected for the patch-clamp study.

Patch-Clamp Recordings and Data Analysis

Whole-cell membrane currents were recorded with an EPC-8 patch-clamp amplifier (HEKA, Lambrecht, Germany). A coverslip with adherent CHO cells was placed on the glass bottom of a recording chamber (0.5λml in volume) mounted on the stage of Nikon Diaphot inverted microscope (Tokyo, Japan). Patch pipettes were prepared from glass capillary tube (Narishige, Tokyo, Japan) by means of a Sutter P-97 micropipette puller (Novato, CA), and the tips were then fire-polished with a microforge. Pipette resistance ranged from 2 to 4 Mω when filled with internal solution. Current recordings were conducted at 34±1°C. Voltage-clamp protocols and data acquisition were controlled by PatchMaster software (version 2.03, HEKA) via an LIH-1600 AD/DA interface (HEKA). Cell membrane capacitance (Cm) was measured in every cell by fitting a single exponential function to capacitive transients elicited by 20 ms voltage-clamp steps from a holding potential of −80 mV.

External Tyrode solution contained (mM): 140 NaCl, 0.33 NaH_2PO_4, 5.4 KCl, 1.8 $CaCl_2$, 0.5 $MgCl_2$, 5.4 glucose, and 5 HEPES, and pH was adjusted to 7.4 with NaOH. The internal